OPEN ACCESS

ORIGINAL ARTICLE

Mechanism of mitochondrial permeability transition pore induction and damage in the pancreas: inhibition prevents acute pancreatitis by protecting production of ATP

Rajarshi Mukherjee,[1,2] Olga A Mareninova,[3] Irina V Odinokova,[3,4] Wei Huang,[1,2,5] John Murphy,[1,2] Michael Chvanov,[1,2] Muhammad A Javed,[1,2] Li Wen,[1,2] David M Booth,[1,2] Matthew C Cane,[2] Muhammad Awais,[1,2] Bruno Gavillet,[6] Rebecca M Pruss,[7] Sophie Schaller,[7] Jeffery D Molkentin,[8] Alexei V Tepikin,[1,2] Ole H Petersen,[9] Stephen J Pandol,[3] Ilya Gukovsky,[3] David N Criddle,[1,2] Anna S Gukovskaya,[3] Robert Sutton,[1,2] and NIHR Pancreas Biomedical Research Unit[1]

▶ Additional material is published online only. To view please visit the journal online (http://dx.doi.org/10.1136/gutjnl-2014-308553).

For numbered affiliations see end of article.

Correspondence to
Professor Robert Sutton, NIHR Liverpool Pancreas Biomedical Research Unit, 5th Floor UCD, Royal Liverpool University Hospital, Daulby Street, Liverpool L69 3GA, UK; r.sutton@liverpool.ac.uk
Anna S. Gukovskaya, UCLA/Veterans Affairs Greater Los Angeles Healthcare System, West Los Angeles Veterans Affairs Healthcare Center, 11301 Wilshire Blvd., Blg. 258, Rm. 340, Los Angeles, California 90073, USA; agukovsk@ucla.edu

Received 2 October 2014
Revised 16 March 2015
Accepted 7 April 2015
Published Online First 12 June 2015

ABSTRACT

Objective Acute pancreatitis is caused by toxins that induce acinar cell calcium overload, zymogen activation, cytokine release and cell death, yet is without specific drug therapy. Mitochondrial dysfunction has been implicated but the mechanism not established.

Design We investigated the mechanism of induction and consequences of the mitochondrial permeability transition pore (MPTP) in the pancreas using cell biological methods including confocal microscopy, patch clamp technology and multiple clinically representative disease models. Effects of genetic and pharmacological inhibition of the MPTP were examined in isolated murine and human pancreatic acinar cells, and in hyperstimulation, bile acid, alcoholic and choline-deficient, ethionine-supplemented acute pancreatitis.

Results MPTP opening was mediated by toxin-induced inositol trisphosphate and ryanodine receptor calcium channel release, and resulted in diminished ATP production, leading to impaired calcium clearance, defective autophagy, zymogen activation, cytokine production, phosphoglycerate mutase 5 activation and necrosis, which was prevented by intracellular ATP supplementation. When MPTP opening was inhibited genetically or pharmacologically, all biochemical, immunological and histopathological responses of acute pancreatitis in all four models were reduced or abolished.

Conclusions This work demonstrates the mechanism and consequences of MPTP opening to be fundamental to multiple forms of acute pancreatitis and validates the MPTP as a drug target for this disease.

Significance of this study

What is already known on this subject?

- Toxins that induce acute pancreatitis cause pancreatic acinar cell calcium overload, intracellular zymogen activation, cytokine release and cell death.
- Mitochondrial matrix calcium overload induces opening of the mitochondrial permeability transition pore (MPTP), a non-specific inner mitochondrial membrane channel that causes loss of mitochondrial membrane potential essential to ATP production.
- Calcium-induced opening of the MPTP occurs in acute pancreatitis, but the mechanism and consequences of this process have not been established.

What are the new findings?

- Toxins that cause acute pancreatitis induce the MPTP in isolated murine and human pancreatic acinar cells via second messenger receptor calcium channel release and mitochondrial calcium but not reactive oxygen species overload, resulting in mitochondrial depolarisation, impaired ATP production and necrosis.
- Pancreatitis toxin-induced MPTP opening causes activation of phosphoglycerate mutase 5, which executes necrosis, and retarded autophagy, which causes accumulation of activated digestive enzymes.
- Specific genetic or pharmacological inhibition of MPTP opening in a diverse range of clinically relevant mouse models dramatically improves all local pancreatic, systemic and distant pulmonary pathological responses.

INTRODUCTION

Pancreatic necrosis, systemic inflammatory response syndrome, multiple organ failure and sepsis are characteristic of severe acute pancreatitis (AP), which results in death of one in four patients and is without specific drug therapy.[1 2] As the pancreatic acinar cell is an initial site of injury,[1 3] commonly initiated by bile or ethanol excess, investigation of its behaviour in response to toxins that induce AP may identify new drug targets. This cell typifies non-excitable exocrine cells with a high secretory turnover heavily dependent on mitochondrial production of ATP.[4] While zymogen activation has

To cite: Mukherjee R, Mareninova OA, Odinokova IV, *et al*. *Gut* 2016;**65**:1333–1346.

Significance of this study

How might it impact on clinical practice in the foreseeable future?

- The demonstration of identical mechanisms in human as in murine pancreatic acinar cells indicates that the findings that establish MPTP opening to be of critical importance in experimental acute pancreatitis are likely to be of major importance in clinical acute pancreatitis.
- This study has shown the effectiveness in experimental acute pancreatitis of several drugs that target molecules that regulate the MPTP and that could be developed for the treatment of clinical acute pancreatitis.
- Translational drug discovery and development programmes that target the MPTP could provide specific, effective treatments for clinical acute pancreatitis.

long been considered the principal mechanism of injury,[1 3] mitochondrial dysfunction has been implicated increasingly,[5–11] presumed consequent upon intracellular calcium overload induced by toxins that include bile acids and ethanol metabolites.[6 11 12] Mitochondrial uptake of calcium drives normal cellular bioenergetics, but high calcium loads induce increasingly drastic responses culminating in necrosis.[13] Mitochondrial matrix calcium overload leads to opening of the mitochondrial permeability transition pore (MPTP), a non-specific channel that forms in the inner mitochondrial membrane allowing passage of particles under 1500 Da, causing loss of mitochondrial membrane potential ($\Delta\psi_m$) essential to ATP production;[13] recent evidence implicates F_0F_1 ATP synthase in MPTP formation.[14 15] MPTP opening is physiological in low conductance mode releasing calcium and reactive oxygen species (ROS) to match metabolism with workload,[16] but pathological in high conductance mode compromising ATP production and inducing cell death;[13] both functions are regulated by the mitochondrial matrix protein peptidyl-prolyl *cis-trans* isomerase (PPI, cyclophilin) D (also known as cyclophilin F).[17]

Previous limited studies found that MPTP opening can occur in pancreatitis;[5 9 18] we found cyclophilin D knockout to ameliorate AP induced by ethanol and cyclosporine,[9] but in a model with no clinical correlate. How the MPTP is induced in pancreatic acinar cells has not been determined, nor what role intracellular calcium might play and whether there are downstream consequences in AP. Therefore, we sought to undertake a novel, wide ranging and detailed study to determine the mechanism and significance of MPTP opening in AP.

We report that MPTP opening is critical to all forms of pancreatitis investigated, causing diminished ATP production, defective autophagy, zymogen activation, cytokine release, phosphoglycerate mutase family member 5 (PGAM5) activation[19] and necrosis. Pharmacological or genetic MPTP inhibition in murine or human pancreatic acinar cells protected $\Delta\psi_m$, ATP production, autophagy and prevented necrosis from pancreatitis toxin-induced calcium release via inositol trisphosphate and ryanodine (IP_3R, RyR) calcium channels. This mechanism was confirmed consistently across four dissimilar, clinically relevant, in vivo models of AP. All characteristic local and systemic pathological responses were greatly reduced or abolished in cyclophilin D knockout mice ($Ppif^{-/-}$)[20] and wild type (Wt) mice treated with MPTP inhibitors, confirming that MPTP opening is a fundamental pathological mechanism in AP.

METHODS

Animals

Cyclophilin D-deficient mice were generated by targeted disruption of the *Ppif* gene[20] and provided by Dr Derek Yellon (University College London, UK) and Dr Michael A Forte (Oregon Health and Sciences University, USA). Transgenic green fluorescent protein (GFP)-LC3 mice[21] were a gift from Dr N Mizushima (Tokyo Medical and Dental University and RIKEN BioResourse Center, Japan). All experiments comparing Wt and $Ppif^{-/-}$ were conducted using C57BL/6 mice; experiments using toxins on Wt cells alone used CD1 mice.

Preparation of isolated pancreatic acinar cells and mitochondria

Normal human pancreata samples (~1 cm×1 cm×1 mm, not devascularised during surgery before removal) were placed in a solution of (mM): 140 NaCl, 4.7 KCl, 1.13 $MgCl_2$, 1 $CaCl_2$, 10 D-glucose, 10 HEPES (adjusted to pH 7.35 using NaOH) at 4°C; sampling to start of cell isolation (or slicing below) was <10 min in every case. All experiments were at room temperature (23–25°C, except where stated) and cells used within 4 h of isolation. Isolation of murine[7] and human[22] pancreatic acinar cells was as described. Isolated murine cells were incubated at 37°C in 199 medium with or without 10 nM cholecystokinin-8 (CCK-8) or 500 μM taurolithocholic acid sulfate (TLCS); drug pretreatment was applied for 30 min. Mitochondria were isolated from mouse pancreata as described.[23]

Confocal fluorescence microscopy

Cells and tissue were viewed using Zeiss LSM510 and LSM710 systems (Carl Zeiss Jena GmbH), typically with a 63x C-Apochromat water immersion objective (aperture at 1.2) after loading with Fluo-4 (3 μM; excitation 488 nm, emission 505 nm) and tetramethyl rhodamine methyl ester (50 nM; excitation 543 nm, emission >550 nm) to assess cytosolic calcium and mitochondrial membrane potential, with simultaneous measurements of NAD(P)H autofluorescence (excitation 351 nm, emission 385–470 nm) to assess mitochondrial metabolism. The protonophore carbonyl cyanide *m*-chlorophenyl hydrazone (CCCP) was applied to dissipate $\Delta\psi_m$ as a positive control. ROS were assessed after loading with 5-chloromethyl-2,7-dichlorodihydrofluorescein diacetate acetyl ester (4.5 μM; excitation 488 nm, emission 505–550 nm) for 10 min at 37°C.[12] R110-aspartic acid amide (20 μM; excitation 488 nm, emission >505 nm) and propidium iodide (PI 1 μM; excitation 488 nm, emission 630–693 nm) were used to assess general caspase activation and plasma membrane rupture. Thirty random fields of view were taken of each isolate and the percentage number of cells displaying caspase activity or PI uptake counted per field, averaged across fields as mean±SEM (minimum three mice/group). PI was used in patched cells (below), as was Mg Green (4 μM, excitation 476 nm, emission 500–550 nm), to monitor intracellular ATP concentrations.[6] Murine pancreas lobules were incubated with/without 500 μM TLCS and stained with Sytox Orange[24] (500 nM, excitation 543 nm, emission >560 nm), which like PI only stains cells with ruptured cell membranes: uptake was determined every two hours by % area tissue stained.

Patch-clamp current recording

The whole-cell configuration was used to record ICl_{Ca} from single cells while recording cytosolic calcium (Fluo-4).[25] Patch-pipettes were pulled from borosilicate glass capillaries

(Harvard Apparatus) with resistance of 2–3 MΩ when filled with a solution of (mM): 140 KCl; 1.5 $MgCl_2$; 2 MgATP; 10 HEPES; 0.1 ethylene glycol tetraacetic acid, pH 7.2. The second messenger IP_3, cyclic ADP ribose (ADPR) or nicotinic acid adenine dinucleotide phosphate (NAADP) was added to the pipette solution at quasi-physiological concentrations (1–10 μM); in some experiments, MgATP was omitted, while in others MgATP was raised to 4 mM. Patched cells were exposed to TLCS (10 μM with second messenger or ACh or CCK-8, otherwise 200 μM) or palmitoleic acid ethyl ester (POAEE, 10 μM) for 20 min then stained with PI. Whole-cell currents were sampled at 10 kHz (EPS8 amplifier and Pulse software, HEKA) from a holding potential of −30 mV, with steps to +10 mV, beyond the reversal potential (0 mV) of the two Ca^{2+}-dependent currents through Cl^- and non-selective cationic channels.[25]

Experimental AP

Caerulein (CER)-AP was induced in male (25–30 g) mice by 7 hourly intraperitoneal injections of 50 μg/kg CER;[26] controls received saline; sacrifice was made 7 h after the first injection for *Ppif*$^{-/-}$ comparisons with Wt, or 12 h for assessment of DEB025 or TRO40303 in Wt. Dosing was determined by prior pharmacokinetic and pharmacodynamic studies (data not shown), which identified optimum regimens of 12 hourly injections of DEB025 at 10 mg/kg or TRO40303 at 3 mg/kg. TLCS-AP was induced as described[27] by retrograde injection of the pancreatic duct with 3 mM TLCS while controls had ductal injection of saline; sacrifice was 24 h later. Fatty acid ethyl ester (FAEE)-AP was induced by 2 hourly intraperitoneal 1.35 g/kg ethanol and 150 mg/kg palmitoleic acid (POA)[11] with controls receiving saline; sacrifice was 24 h later. Choline-deficient ethionine-supplemented (CDE)-AP was induced in young female mice (14–15 g) fasted overnight and fed CDE[28] or regular chow for 48 h, then sacrificed.

Histopathology

Pancreatic necrosis was measured on H&E sections as described and apoptosis with TUNEL.[7] Two independent, blinded investigators scored oedema, leucocyte infiltration and necrosis (0–3) on ×10 high-power fields/slide/mouse. Scores were summated (mean±SEM ≥6 mice/group; ≥4 for CDE-AP).

Statistical analysis

Data are presented as mean±SEM. Analysis was by two-tailed Student's t test or χ^2 test, with p values <0.05 considered significant.

Study approval

For preparation of pancreas tissue slices and lobules, measurement of isolated mitochondrial responses, electron microscopy, immunofluorescence, further assessment of disease parameters in experimental AP and details of chemicals and reagents, see online supplementary materials.

RESULTS

Pharmacological MPTP inhibition prevents pancreatitis toxin-induced mitochondrial impairment and necrotic cell death pathway activation

First, we tested the effect of known MPTP inhibitors on toxin-induced changes in pancreatic acinar cells using cyclosporin A (CYA), which binds to and inhibits cyclophilin D, or bongkrekic acid (BKA), which favours the closed conformation of adenine nucleotide translocase.[29] We used murine cells hyperstimulated with CCK-8[18 30] to induce cytosolic and mitochondrial calcium overload,[6 12] and found loss of $\Delta\psi_m$[7 18] causing decreases in NAD(P)H (figure 1A), reflecting declining ATP production.[4] The bile acid TLCS[31] induced similar changes (figure 1B). Both CYA and BKA prevented losses of $\Delta\psi_m$ and NAD(P)H. TLCS-induced mitochondrial impairment was completely prevented by the calcium chelator 1,2-bis(o-aminophenoxy) ethane-N,N,N′,N′-tetraacetic acid and was dose dependent (see online supplementary figure S1). We then tested D-MeAla[3]-EtVal[4]-cyclosporine (Alisporivir, DEB025), which inhibits cyclophilin D but is not immunosuppressive[29] and 3,5-Seco-4-nor-cholestan-5-one oxime-3-ol (TRO40303), which also inhibits MPTP opening;[32] both prevented decreases of $\Delta\psi_m$ in murine and freshly isolated human pancreatic acinar cells (figure 1C). Marked cell death pathway activation was induced by CCK-8 and TLCS; whereas caspase activation occurred in the presence of CYA or BKA, PI uptake was largely prevented (figure 1D). Marked protection from TLCS in human pancreatic acinar cells[22] and human pancreas slices followed pretreatment with CYA, DEB025 and TRO40303 (figure 1E, F).

Genetic MPTP inhibition prevents pancreatitis toxin-induced mitochondrial impairment and necrotic cell death pathway activation

Cytosolic calcium changes were significantly less marked in pharmacologically treated than control cells (seen with CYA and BKA due to an initial release of calcium from cell stores, but not with DEB025 or TRO40303, see online supplementary figure S1), which might reduce mitochondrial calcium loading, so we examined effects of genetic deletion (*Ppif*$^{-/-}$) of cyclophilin D.[20] Comparison of *Ppif*$^{-/-}$ and Wt (C57BL/6) cells showed CCK-8-induced cytosolic calcium elevations were similar, but in *Ppif*$^{-/-}$ calcium clearance was significantly faster (mean±SE area under curve (F/F_0×s) 199.61±26.45 vs 262.35±30.73 in Wt, $p<0.05$), a function of calcium ATPase pumps (figure 2A, left). In Wt cells, $\Delta\psi_m$ and NAD(P)H fell steadily, but not in *Ppif*$^{-/-}$ (figure 2A, middle and right). TLCS induced similar changes (figure 2B) with significantly faster calcium clearance in *Ppif*$^{-/-}$ cells (243.82±32.34 vs 378.92±45.98 in Wt, $p<0.05$), despite little difference detected in mitochondrial calcium loading (figure 2C, left). Subsequent experiments demonstrated no difference between *Ppif*$^{-/-}$ and Wt cells in store-operated calcium entry or plasma membrane ATPase calcium pump extrusion (see online supplementary figure S1), consistent with more effective ATP supply in *Ppif*$^{-/-}$ compared with Wt cells subjected to CCK-8- or TLCS-induced calcium overload. As TLCS-induced ROS increases promote apoptosis not necrosis of pancreatic acinar cells,[12 23] we tested whether ROS increases are greater in *Ppif*$^{-/-}$ cells and found no differences from Wt (figure 2C, middle), ruling this out as a protective mechanism. Ethanol and POA, which form the toxic FAEE POAEE that induces AP,[11] also caused marked falls of $\Delta\psi_m$ in Wt not *Ppif*$^{-/-}$ cells (figure 2C, right). There were marked effects of *Ppif*$^{-/-}$ on PI uptake but little on general caspase activation (figure 2D), consistent with a minor role for MPTP opening in pancreatic acinar cell apoptosis.[7 23] In keeping, cytosolic cytochrome *c* release was seen in both *Ppif*$^{-/-}$ and Wt cells after hyperstimulation, although less in *Ppif*$^{-/-}$ cells (figure 2E). We also tested pancreatic lobules, more closely representing events in vivo, and found necrotic pathway activation (Sytox Orange uptake)[24] markedly inhibited in *Ppif*$^{-/-}$ (figure 2F).

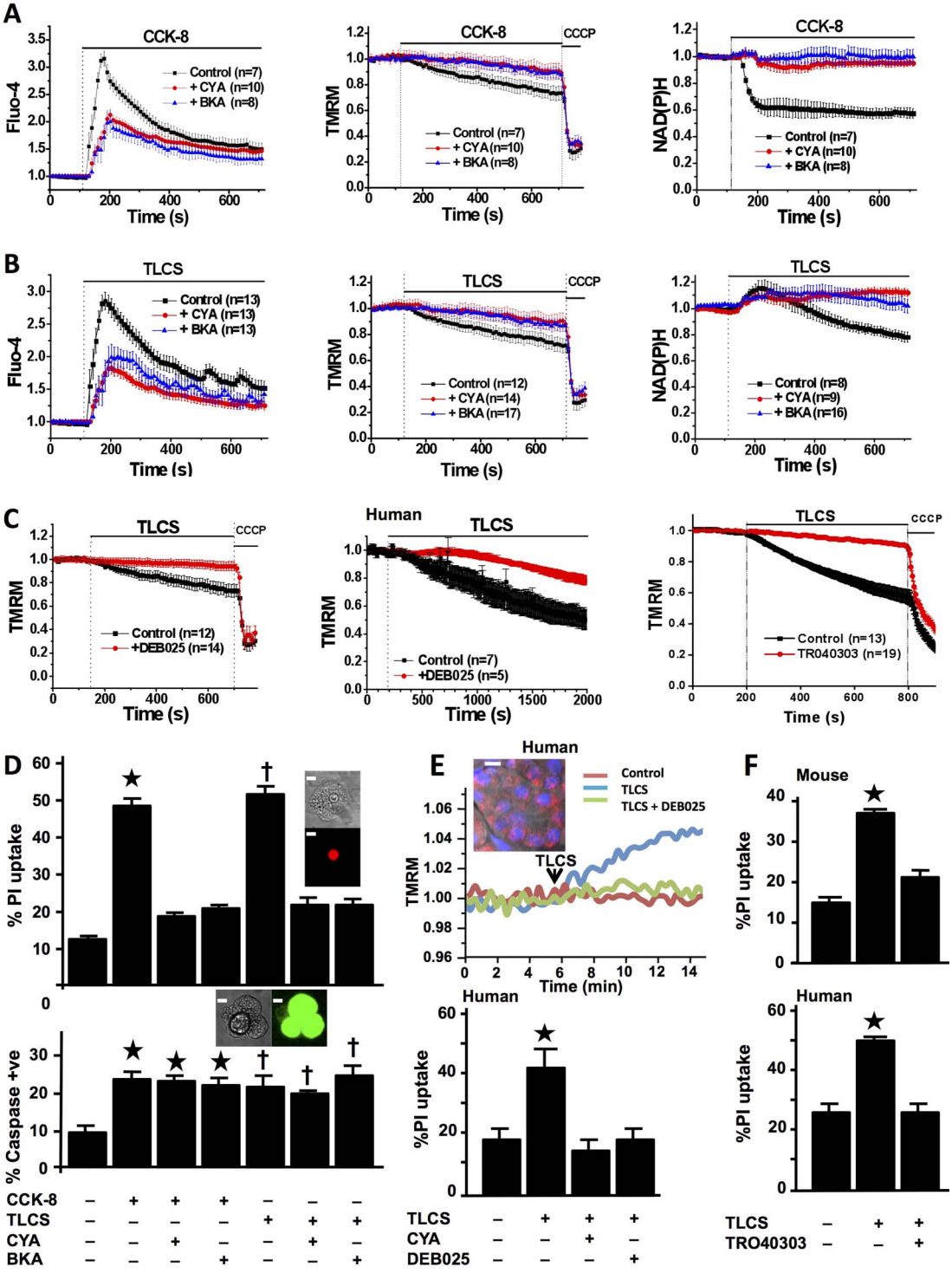

Figure 1 Mitochondrial permeability transition pore (MPTP) inhibitors prevent mitochondrial impairment and necrosis of freshly isolated murine and human pancreatic acinar cells (confocal fluorescence; mean±SEM ratio to basal, F/F_0; n=no. of experiments). (A) Cholecystokinin-8 (CCK-8) (10 nM) induced large cytosolic calcium elevations (Fluo-4, left), falls in $\Delta\psi_m$ (tetramethyl rhodamine methyl ester, TMRM; positive control, protonophore carbonyl cyanide *m*-chloro phenyl hydrazone, CCCP, middle) and NAD(P)H autofluorescence (right), showing protection of $\Delta\psi_m$ and NAD(P)H by cyclosporin A (CYA, 5 μM) or bongkrekic acid (BKA, 50 μM) (pretreatment for 30 min at room temperature during loading of fluorescent dyes). (B) Taurolithocholic acid sulfate (TLCS) (500 μM) induced similar changes in calcium, $\Delta\psi_m$ and NAD(P)H, with similar protection by CYA and BKA. (C) Protection of $\Delta\psi_m$ from TLCS (500 μM) by pretreatment with DEB025 (100 nM) in murine (left) and human (middle) pancreatic acinar cells, and with TRO40303 (10 μM, right) in murine cells. (D) CYA or BKA protected cells from early plasma membrane rupture (top, % cells showing propidium iodide (PI) uptake as inset; *p<0.05 CCK-8 vs control or with inhibitor; †p<0.05 TLCS vs control or with inhibitor) but not from caspase activation (bottom, % cells showing general caspase substrate fluorescence as inset; *p<0.05, control vs all CCK-8 groups; †p<0.05 control vs all TLCS groups; white bars=5 μm). (E) Typical rise in TMRM dequench fluorescence[31] emitted by normal fresh human pancreatic tissue slice in response to TLCS (500 μM) and protection by DEB025 (100 nM; upper panel; inset shows confocal image of human pancreatic tissue slice (mitochondrial (TMRM, red) and nuclear (Hoescht, blue) fluorescent dyes, white bar=15 μm). Lower panel shows protection from TLCS-induced PI uptake in human pancreatic acinar cells by CYA (100 nM) or DEB025 (100 nM, bottom) and (F) murine (top) and human (bottom) cells by TRO40303 (10 μM) (*p<0.05 TLCS vs control or with CYA, DEB025 or TRO40303).

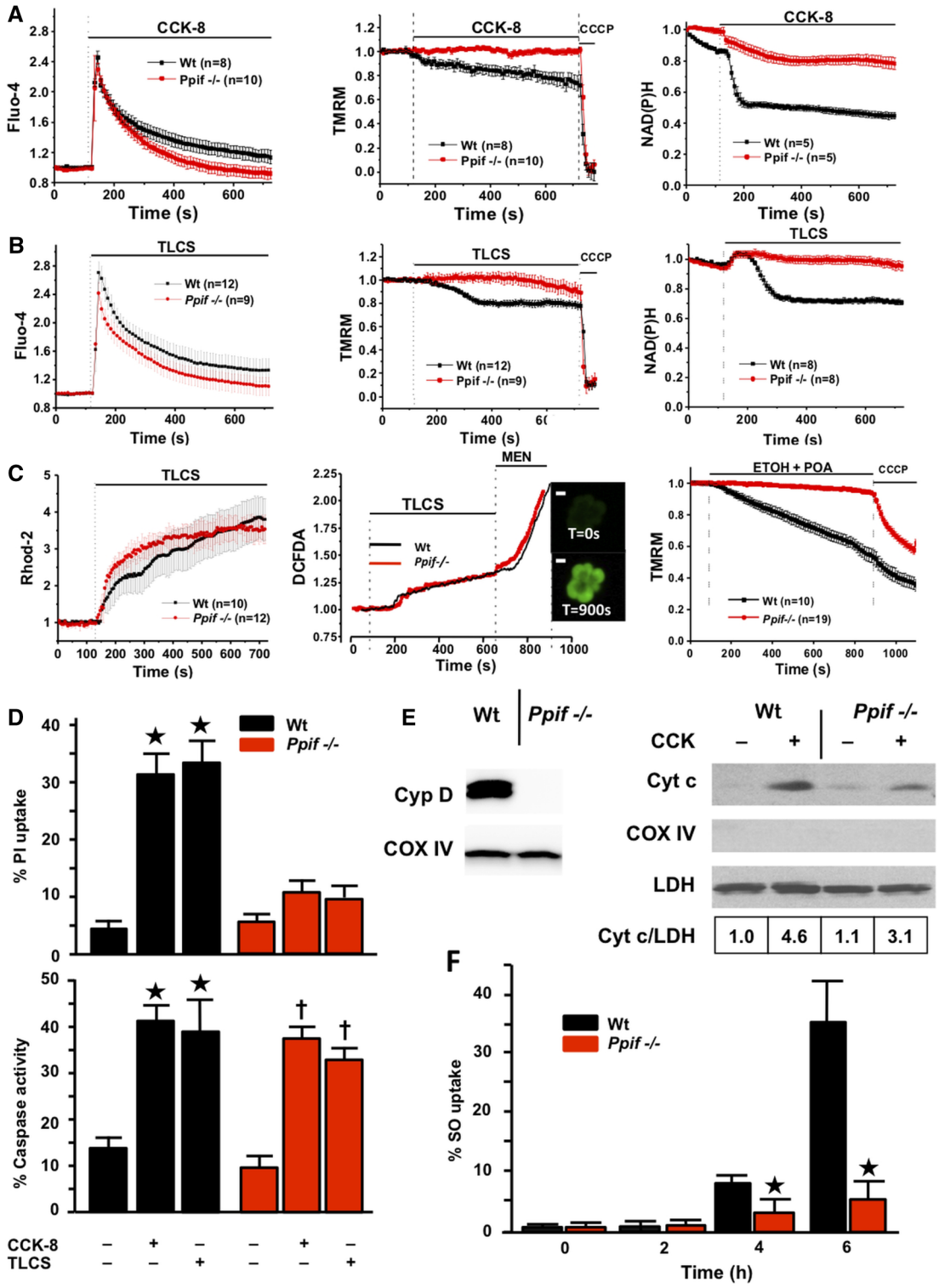

Figure 2 Genetic ablation of cyclophilin D (*Ppif*$^{-/-}$) protects pancreatic acinar cells from pancreatitis toxins (fluorescence mean±SEM, F/F_0). (A) Cholecystokinin-8 (CCK-8) (10 nM) induced cytosolic calcium elevations (Fluo-4, left) in Wt (C57BL/6) and *Ppif*$^{-/-}$ cells, with faster clearance in *Ppif*$^{-/-}$; $\Delta\psi_m$ (TMRM, middle) and NAD(P)H (right) were preserved in *Ppif*$^{-/-}$ not wild type (Wt) cells. (B) Taurolithocholic acid sulfate (TLCS) (500 μM) induced similar calcium changes, clearing faster in *Ppif*$^{-/-}$; whereas $\Delta\psi_m$ and NAD(P)H were preserved in *Ppif*$^{-/-}$ not Wt. (C) TLCS (500 μM) induced similar mitochondrial calcium elevations (Rhod-2, left) in *Ppif*$^{-/-}$ and Wt cells, as well as similar reactive oxygen species (ROS) elevations (DCFDA, middle) in *Ppif*$^{-/-}$ and Wt cells (menadione, MEN oxidant control); insets show ROS-sensitive DCFDA cell fluorescence (white bars=10 μm); ethanol (ETOH, 10 mM) and palmitoleic acid (POA, 20 μM) induced falls of $\Delta\psi_m$ (right) in Wt not *Ppif*$^{-/-}$ cells. (D) Significantly increased propidium iodide (PI) uptake in Wt not *Ppif*$^{-/-}$ cells after CCK-8 (10 nM) or TLCS (500 μM) (top, *p<0.05 toxin in Wt versus no toxin or toxin in *Ppif*$^{-/-}$), but similar general caspase activation (bottom, *p<0.05 no toxin vs each toxin group). (E) Cyclophilin absence in *Ppif*$^{-/-}$ pancreas (immunoblot, left) and cytochrome *c* (Cyt c) cytosolic fraction immunoblots (densitometry normalised to lactate dehydrogenase (LDH), Cox IV to rule out mitochondrial contamination, right) showed Cyt c release after CCK-8 by Wt and less by *Ppif*$^{-/-}$ mitochondria. (F) Necrotic cell death pathway activation (Sytox Orange; SO) from TLCS (500 μM) was delayed in *Ppif*$^{-/-}$ vs Wt pancreas lobules (*p<0.05).

Pancreatitis toxin-induced acinar cell MPTP opening causes collapse of ATP production and necrotic cell death pathway activation via second messenger receptor calcium channel release

As bile acids and FAEEs induce global, prolonged acinar cytosolic calcium release via IP_3R and RyR calcium channels,[6 33] which causes zymogen activation[34 35] dependent on sustained calcium entry,[36] we sought to determine how toxin-induced calcium release causes mitochondrial injury and pancreatic acinar cell death. Using patch clamp technology and confocal microscopy, we observed typical apical stimulus-secretion coupling calcium signals elicited by IP_3 (1–10 μM), matched by calcium-activated Cl^- currents[4 25] (ICl_{Ca}). These signals were promptly transformed into global, prolonged (>30 s) cytosolic calcium elevations by low concentrations of TLCS (10 μM, 31 of 33 cells, figure 3A, B) or POAEE (10 μM, 34 of 37 cells, see online supplementary figure S2), followed by PI uptake in Wt cells (figure 3B and see online supplementary table). Application of the non-specific IP_3R antagonist caffeine[6] inhibited calcium changes and ICI_{Ca} from both toxins, preventing PI uptake (22 of 22 cells, figure 3A, see online supplementary figure S2 and table), demonstrating dependence of toxic transformation on IP_3Rs. Necrotic cell death pathway activation was entirely dependent on calcium influx (figure 3B and see online supplementary figure S2). Typical calcium signals and ICI_{Ca} elicited by the RyR ligand cyclic ADPR (cyclic ADPR, 10 μM)[25] were transformed by TLCS (10 μM), not POAEE; those elicited by NAADP (100 nM)[25] were transformed by POAEE (10 μM), not TLCS (see online supplementary figure S2). To model events in vivo, quasi-physiological concentrations of CCK-8 or acetylcholine (ACh) were tested with both toxins, again resulting in toxic transformation (24 of 24 cells, no patch pipette, figure 3C, see online supplementary figure S2 and table). Without any second messenger or secretagogue, higher toxin concentrations (TLCS, 200 μM, figure 3D; POAEE 100 μM, data not shown; both inhibited by caffeine) were required to induce global, prolonged calcium elevations. All protocols that induced such elevations sustained by external calcium entry resulted in PI uptake in Wt cells (56 of 60 cells, ≥5 cells with each protocol; figure 3B–D); patched ATP resulted in more efficient calcium clearance and prevented all PI uptake (46 of 46 Wt cells, ≥4 cells with each protocol; $p<0.0001$), and ATP depletion from toxic transformation without patched ATP was confirmed using Mg Green (figure 3C, see online supplementary figure S2 and table). In all *Ppif*$^{-/-}$ cells, there was significantly more efficient calcium clearance, reduced ICI_{Ca} and return to baseline levels with no PI uptake, despite no patched ATP (IP_3 and TLCS, 10 μM, 17 of 17 cells; TLCS, 200 μM, 7 of 7 cells, figure 3D). These findings identify a primary role for second messenger calcium channel release in MPTP opening induced by pancreatitis toxins, resulting in declining ATP production and necrosis.

The MPTP determines the sensitivity of pancreatic mitochondria to calcium overload and PGAM5 induction

To confirm the role of calcium overload in pancreatic acinar cell MPTP opening, we examined responses of isolated *Ppif*$^{-/-}$ and Wt pancreatic mitochondria to external calcium. *Ppif*$^{-/-}$ and Wt pancreatic mitochondria demonstrated similar capacity to generate ATP, as measured by respiration rate in response to ADP (respiratory control ratio) >3 in the presence of succinate[23] (figure 4A). Both types of mitochondria maintained $\Delta\psi_m$ in zero or 0.6 μM clamped, free ionised calcium for 10 min; in 1.3 μM calcium Wt $\Delta\psi_m$ collapsed, whereas *Ppif*$^{-/-}$ $\Delta\psi_m$ was maintained. While Wt $\Delta\psi_m$ was lost after one addition of 25 μM $CaCl_2$, *Ppif*$^{-/-}$ $\Delta\psi_m$ was lost after five successive additions (figure 4B, C). *Ppif*$^{-/-}$ pancreatic mitochondria released only 35% less cytochrome *c* than Wt in 1.3 μM calcium (figure 4D), consistent with a modest contribution from MPTP opening to cytochrome c release. To further assess the significance of MPTP opening and falls in $\Delta\psi_m$, we measured levels of PGAM5, a mitochondrial executor of necrosis.[19] Falls in $\Delta\psi_m$ cause PGAM5 cleavage from the inner mitochondrial membrane,[37] and increases in PGAM5 promote necrosis, facilitating mitochondrial fission.[19] After induction of CER-AP, PGAM5 was increased in Wt but significantly less in *Ppif*$^{-/-}$ pancreata (figure 4E), indicating a mitochondrial mechanism for necrosis induced by calcium overload in AP. These changes were associated with marked ballooning of and loss of cristae in Wt but not *Ppif*$^{-/-}$ pancreatic acinar mitochondria in CER-AP (figure 4F).

The MPTP mediates zymogen activation through impaired autophagy

Since zymogen activation is considered essential to AP and relates to disease severity,[1 38–40] we sought to determine whether and how this is MPTP dependent. We found CCK-8-induced trypsin activity significantly inhibited in *Ppif*$^{-/-}$ compared with Wt (figure 5A), despite no differences in the amount of trypsinogen (or amylase) between Wt and *Ppif*$^{-/-}$ mice pancreata (figure 5B; nor cathepsin B, Bcl-xL or Bcl-2, data not shown). This finding indicates that MPTP opening contributes to pathological, intra-acinar zymogen activation. Zymogen activation depends on intracellular calcium overload[30] and accumulation of activated zymogens in AP is due to impaired autophagy.[41] We therefore measured levels of microtubule-associated protein 1A/1B-light chain 3 (LC3), which in autophagy is converted from cytosolic LC3-I to lipidated LC3-II and recruited into autophagosomal membranes, and levels of sequestosome 1 (SQSTM1, p62), which sequesters ubiquitinated protein aggregates to autophagosomes; when autophagosomes fuse with lysosomes, both LC3-II and p62 are degraded.[42] Following induction of CER-AP that features marked falls in ATP production, acinar cell vacuolisation and zymogen activation,[7 38 43] significant increases in LC3-II and p62 occurred in Wt pancreata, showing retarded autophagy consistent with previous data.[41] Increases in LC3-II and p62 were significantly attenuated in *Ppif*$^{-/-}$ mice (figure 5C–E), indicating more efficient autophagy.[42] We confirmed the role of MPTP opening in defective autophagy using GFP LC3 mice,[21] crossed with *Ppif*$^{-/-}$ mice. Analysis of LC3 puncta (autophagic vacuoles, figure 5F) as well as increases in LC3-II and p62 in GFP-LC3 versus GFP-LC3×*Ppif*$^{-/-}$ mice (≥3 mice/group, data not shown) confirmed significant attenuation from genetic inhibition of the MPTP.

Genetic or pharmacological MPTP inhibition sustains ATP production and confers striking protection from experimental AP

To determine comprehensively the significance of these mechanisms in vivo, we compared responses of *Ppif*$^{-/-}$ versus Wt mice in four dissimilar models of AP: CER-AP, TLCS pancreatic ductal infusion[27] (TLCS-AP), ethanol with POA[11] (FAEE-AP) and CDE-AP diet.[28] These models represent the whole spectrum of human AP, including the commonest clinical aetiologies (gallstones and ethanol) and extending from mild to lethal disease. In all models, characteristic changes occurred in serum amylase and interleukin-6 (IL-6), pancreatic trypsin and myeloperoxidase, pancreatic ATP and histopathology (figures 6 and 7, see

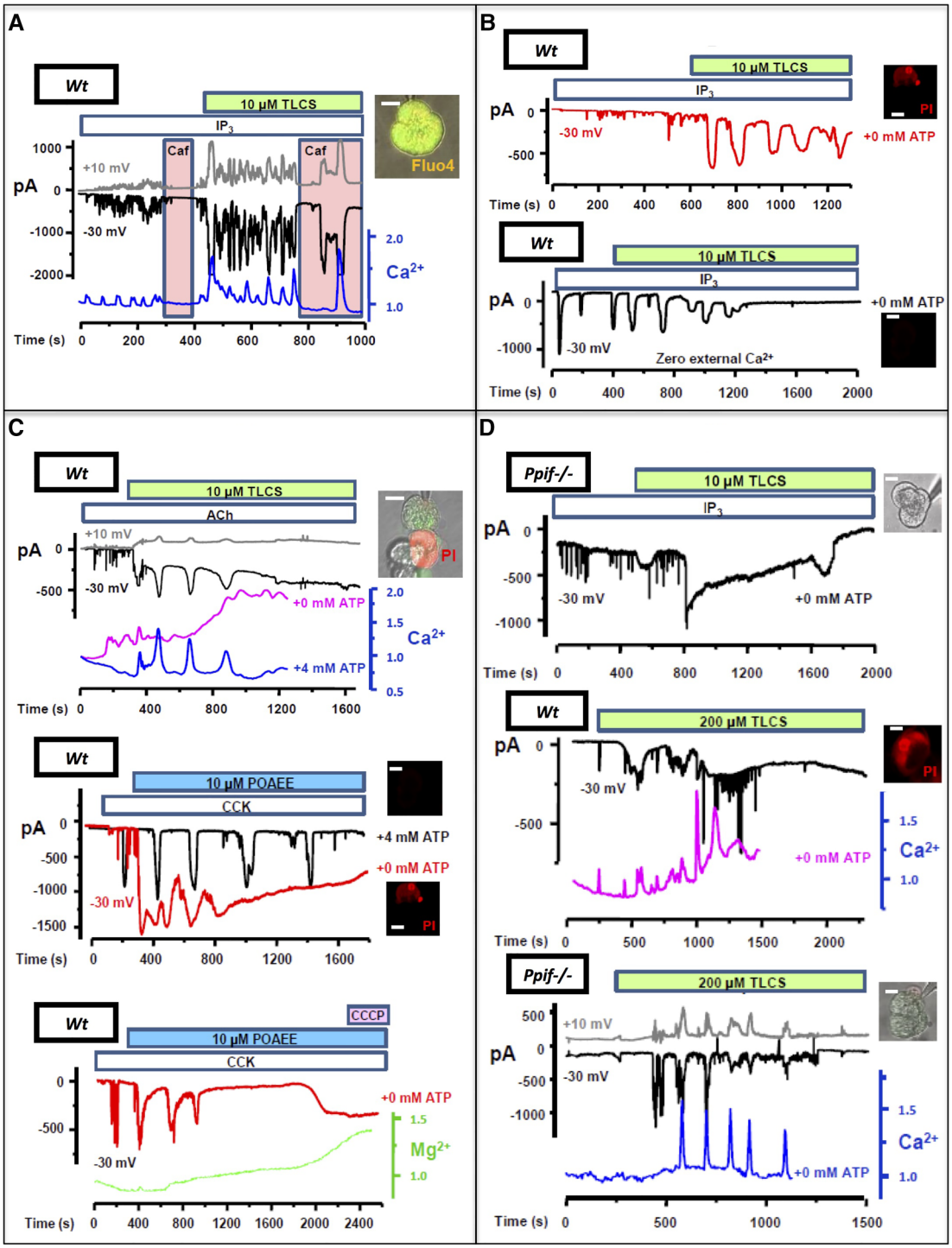

Figure 3 Pancreatitis toxins accelerate calcium release via second messenger receptors causing collapse of ATP production in wild type (Wt) not *Ppif*$^{-/-}$ cells (insets, representative cells, green Fluo-4 and/or red propidium iodide (PI) fluorescence, white bars=10 μm). (A) Typical calcium spikes (Fluo-4, F/F_0, blue) elicited by patched IP_3 (1–10 μM) were transformed into global, prolonged elevations upon Taurolithocholic acid sulfate (TLCS) (10 μM) application, matched by ICl_{Ca} and non-specific cation currents (−30 mV, black and +10 mV, grey; inset patched cell top), inhibited by caffeine (Caf, pink); (B) top plot: toxic transformation (ICl_{Ca} red, no caffeine) showing PI uptake; bottom plot: without external calcium, transformed signals decreased then disappeared (ICl_{Ca} black, no PI uptake). (C) Top plot: toxic transformation of acetylcholine (Ach) (20 nM) signals by TLCS (10 μM), reduced by pipette ATP (4 mM) preventing PI uptake in patched (ICl_{Ca} and blue calcium trace) but not adjacent (purple calcium trace) cell; middle plot: toxic transformation of cholecystokinin-8 (CCK-8) (1–5 pM) signals by palmitoleic acid ethyl ester (POAEE, 10 μM) (red ICl_{Ca}) caused PI uptake, prevented by pipette ATP (black ICl_{Ca}, two recordings superimposed); bottom plot: ATP decline (Mg Green; rise indicates increased ADP:ATP ratio) following toxic transformation (3 pM CCK-8 with 10 μM POAEE; carbonyl cyanide m-chlorophenyl hydrazone induced no further ATP decline). (D) Top plot: representative trace showing transformation of IP_3- (1–10 μM) elicited signal by TLCS (10 μM) did not induce PI uptake in *Ppif*$^{-/-}$ cells, without supplementary ATP; middle plot: TLCS (200 μM) alone induced PI uptake in Wt; bottom plot: TLCS (200 μM) did not induce PI uptake in *Ppif*$^{-/-}$ cells.

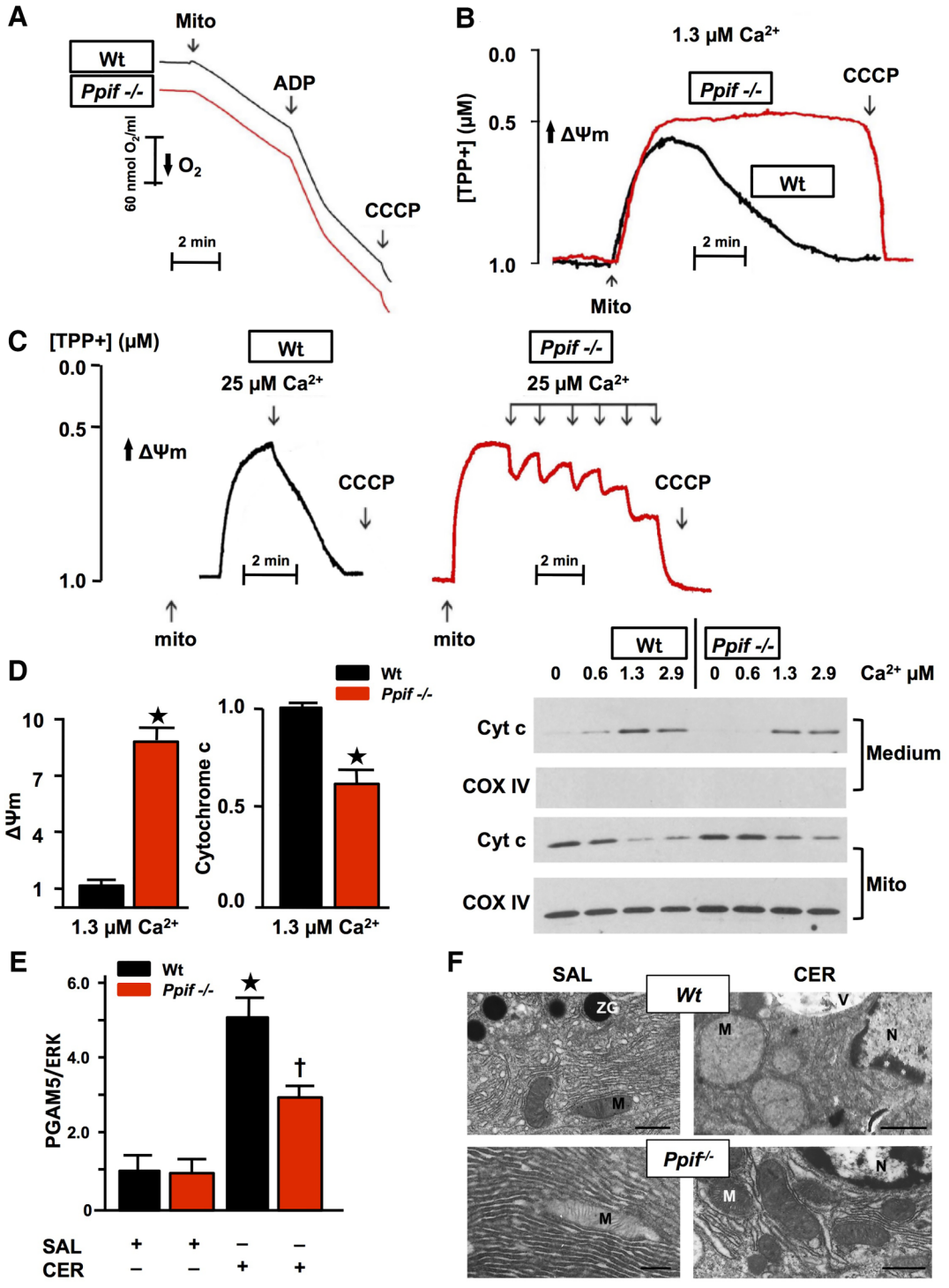

Figure 4 Genetic mitochondrial permeability transition pore (MPTP) inhibition confers resistance of pancreatic mitochondria to calcium-induced loss of $\Delta\psi_m$ and PGAM5 induction. (A) Representative Clark-type electrode measurement of oxygen consumption showed no difference between wild type (Wt) and *Ppif*$^{-/-}$ mitochondria (Mito; succinate=10 mM, ADP=200 µM, carbonyl cyanide m-chlorophenyl hydrazone (CCCP)=2 µM). (B) Typical TPP^+-selective electrode measurement of $\Delta\psi_m$ with succinate (10 mM) in free ionised calcium clamped at 1.3 µM (calcium/ethylene glycol tetraacetic acid buffers) for 10 min and (C) during pulses of calcium (25 µM), showing resistance of *Ppif*$^{-/-}$ mitochondria to loss of $\Delta\psi_m$. (D) $\Delta\psi_m$ (TPP^+-selective electrode, left) and cytochrome *c* (Cyt c; densitometry from Medium immunoblot, right) in the same preparations, normalised to Wt. *Ppif*$^{-/-}$ pancreatic mitochondria release Cyt c but less than Wt (*p<0.05, means±SEM from >3 preparations), as shown in representative Cyt c immunoblot of medium and mitochondrial pellet (Mito, Cox IV confirmed separation and equal protein loading). (E) Increase in PGAM5 in Wt caerulein acute pancreatitis (CER-AP) pancreata was significantly reduced in *Ppif*$^{-/-}$ with representative immunoblot (re-probed for ERK1/2 to confirm equal loading; each lane from an individual animal; 4–6 mice per group; densitometry of PGAM5 as ratio of band intensities to ERK in each sample normalised to saline-treated Wt controls, means±SEM; *p<0.01 CER-AP in Wt vs Wt controls, †p<0.05 CER-AP in *Ppif*$^{-/-}$ vs CER-AP in Wt). (F) Electron micrographs of pancreata showing Wt and *Ppif*$^{-/-}$ pancreatic acinar cells after induction of CER-AP compared with saline (SAL) controls. Wt pancreatic acinar mitochondria are markedly swollen with loss of cristae in CER-AP compared with normal morphology of *Ppif*$^{-/-}$ pancreatic acinar mitochondria in CER-AP and in both Wt and *Ppif*$^{-/-}$ saline controls (M, mitochondrion; N, nucleus; V, vacuole; ZG, zymogen granule; black bars 1 µm except top right, 2.5 µm).

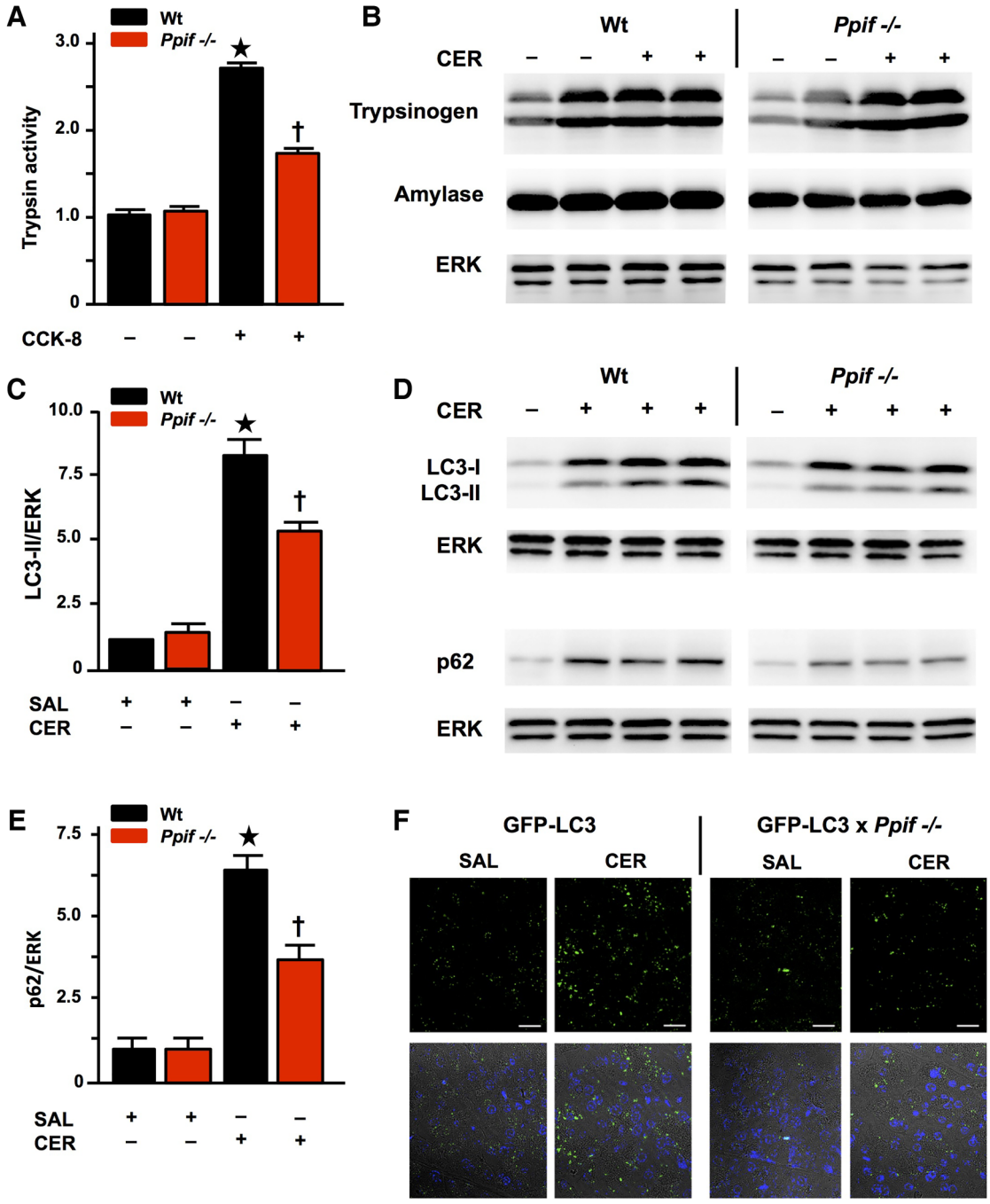

Figure 5 Pancreatitis autophagy impairment and trypsinogen activation are attenuated by genetic mitochondrial permeability transition pore (MPTP) inhibition (*Ppif*$^{-/-}$). (A) Trypsin activity (normalised) following cholecystokinin-8 (CCK-8) (10 nM) hyperstimulation inhibited in *Ppif*$^{-/-}$ vs wilt-type (Wt) cells (mean±SEM 6 cell preparations; *p<0.05 Wt CCK-8 vs Wt controls; †p<0.05 *Ppif*$^{-/-}$ CCK-8 vs Wt CCK-8). (B) Trypsinogen and amylase content similar in unstimulated and caerulein acute pancreatitis (CER-AP) Wt vs *Ppif*$^{-/-}$ pancreata (immunoblot; re-probed for ERK1/2 to confirm equal loading; each lane from an individual animal). (C) Densitometry of LC3-II with (D) representative immunoblots of LC3-II and p62 with (E) densitometry of p62 showing increased levels of these proteins in Wt CER-AP that were both significantly attenuated in *Ppif*$^{-/-}$ mice, indicating more efficient autophagic flux (immunoblots re-probed for ERK1/2 to confirm equal loading; each lane from an individual animal; 4–6 mice per group; densitometry of LC3-II or p62 as ratios of band intensities to ERK in each sample normalised to saline-treated Wt controls, means±SEM; *p<0.01 CER-AP in Wt vs Wt controls, †p<0.05 CER-AP in *Ppif*$^{-/-}$ vs CER-AP in Wt). (F) Representative images showing attenuation of CER-AP-induced increases in LC3-II puncta by genetic MPTP inhibition in green fluorescent protein (GFP)-LC3×*Ppif*$^{-/-}$ compared with GFP-LC3 transgenic mice (upper panels show LC3 puncta in saline-treated pancreas and CER-AP for both strains; lower panels show addition of nuclear stain 4′,6-diamidino-2-phenylindole (DAPI)).

online supplementary figures S3 and S4). In contrast, all pathological responses were greatly inhibited in *Ppif*$^{-/-}$ animals, including lung myeloperoxidase and IL-6, which mediates lung injury and lethality.[44] In Wt, DEB025 (10 mg/kg) or TRO40303 (3 mg/kg) administered 2 h after the start of hyperstimulation in CER-AP (figure 6C, D, see online supplementary figure S3) or 1 h after induction of TLCS-AP (figure 7) markedly reduced or abolished all pathological changes. Protection in TLCS-AP was close to complete: all changes in *Ppif*$^{-/-}$ mice or Wt (C57BL/6) mice treated with DEB025 or TRO40303 were no or minimally

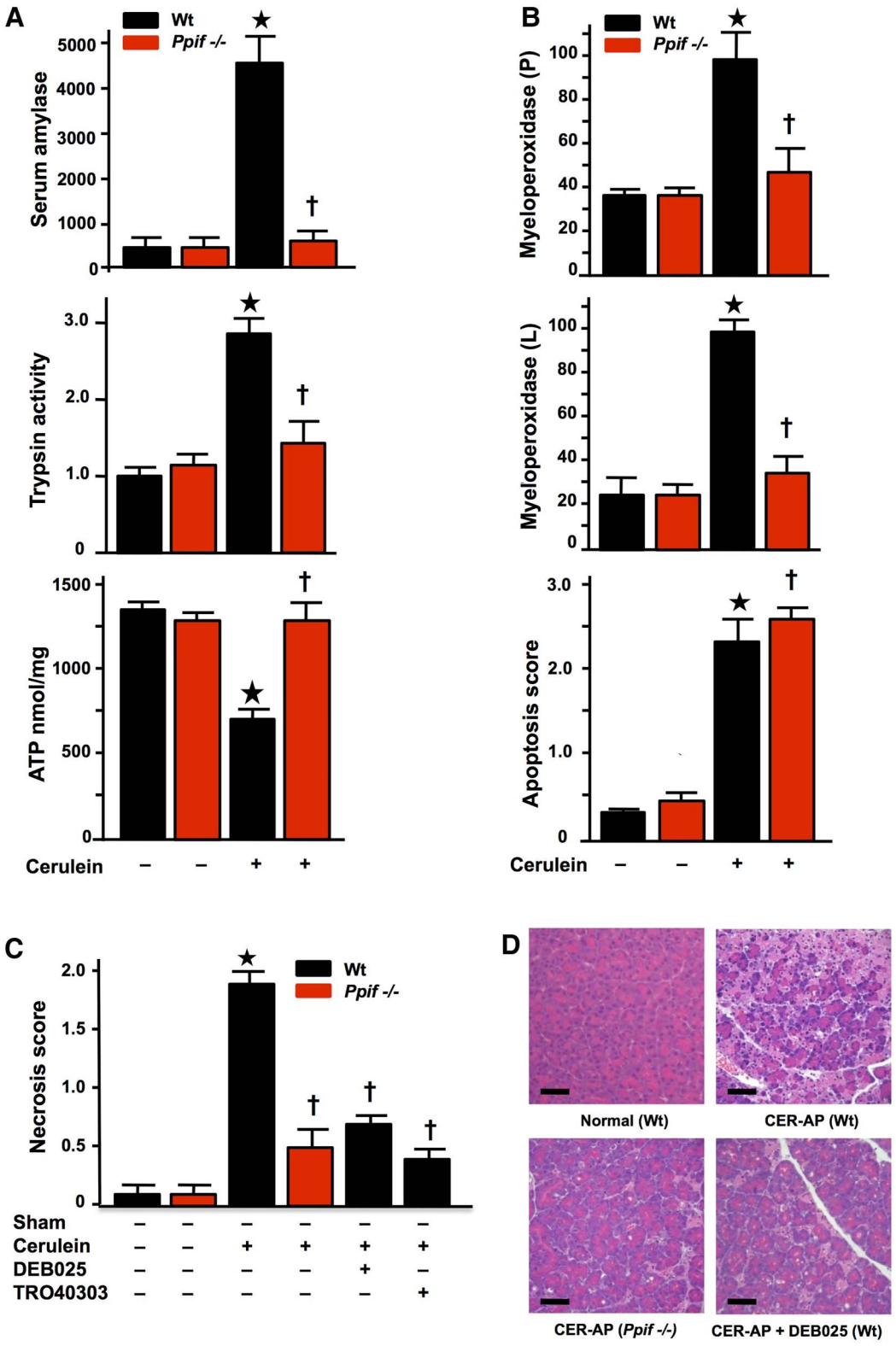

Figure 6 Genetic and pharmacological mitochondrial permeability transition pore (MPTP) inhibition markedly reduces the severity of caerulein acute pancreatitis (CER-AP). (A) CER-AP resulted in substantial elevations of serum amylase (U/L) and pancreatic trypsin (normalised to wild type (Wt) saline controls) with substantial reduction in pancreatic ATP content in Wt (*p<0.05) but not *Ppif*$^{-/-}$ mice (†p<0.05 vs CER-AP in Wt). (B) CER-AP resulted in substantial elevations of pancreatic (P) and lung (L) myeloperoxidase activity (normalised to CER-AP in Wt at 100) in Wt (*p<0.05) but not *Ppif*$^{-/-}$ mice (†p<0.05 vs CER-AP in Wt), while apoptosis scores were significantly increased in CER-AP in both Wt (*p<0.05 vs either control) and *Ppif*$^{-/-}$ (†p<0.05 vs either control). (C) Necrosis scores in CER-AP were substantially reduced in *Ppif*$^{-/-}$ and Wt with DEB025 (10 mg/kg intraperitoneal with third injection of caerulein) or TRO40303 (3 mg/kg intraperitoneal at same time points) compared to Wt with no treatment (all values means±SEM from ≥6 mice per group in all experiments; *p<0.01 CER-AP in Wt vs Wt controls; †p<0.05 CER-AP in *Ppif*$^{-/-}$ or Wt with DEB025 or TRO40303 vs CER-AP in Wt). (D) Normal pancreatic histology (Wt no treatment) contrasted with CER-AP in Wt, *Ppif*$^{-/-}$ or Wt treated with DEB025, showing extensive oedema, necrosis and inflammatory cell infiltration in Wt but not *Ppif*$^{-/-}$ and not in Wt with DEB025 (H&E, black bars=50 μm).

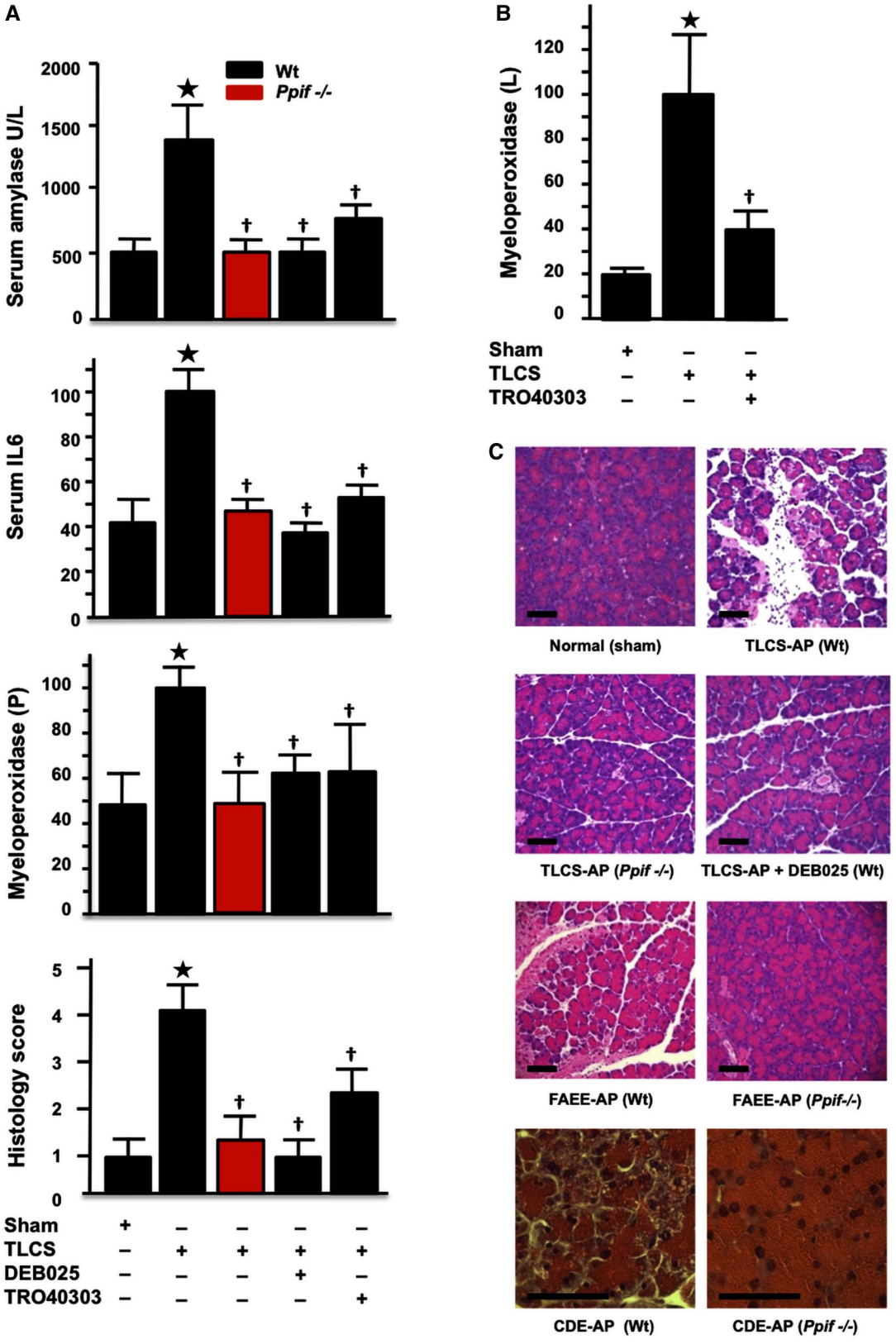

Figure 7 Genetic or pharmacological mitochondrial permeability transition pore (MPTP) inhibition abolishes or markedly attenuates biochemical and histological responses of taurolithocholic acid sulfate acute pancreatitis (TLCS-AP), fatty acid ethyl ester (FAEE)-AP and choline-deficient ethionine-supplemented (CDE)-AP. (A) Characteristic elevations in TLCS-AP of serum amylase (U/L), interleukin-6 (pg/mL), pancreatic (P) myeloperoxidase activity (normalised to TLCS-AP in wild type (Wt) at 100) and histology scores (*p<0.05 for all elevations vs sham controls) were all significantly reduced in *Ppif*$^{-/-}$ or in Wt treated with DEB025 or TRO40303 (†p<0.05 vs TLCS-AP in Wt without treatment). (B) Characteristic elevations in lung (L) myeloperoxidase activity (normalised to TLCS-AP in Wt at 100; *p<0.05 vs sham controls) were significantly reduced in Wt treated with TRO40303 (†p<0.05 vs TLCS-AP in Wt without treatment). (E) Representative histology showing protective effects of *Ppif*$^{-/-}$ in TLCS-AP, of DEB025 on TLCS-AP in Wt and of *Ppif*$^{-/-}$ in FAEE-AP and CDE-AP.

different from sham controls (figure 7). These findings demonstrate that inhibition of MPTP opening confers striking local and systemic protection from pancreatitis. The further new finding of relative independence of apoptotic processes from the MPTP (figure 6B) confirmed that apoptosis is not a major contributor to the pathological responses of AP,[26] unless it is massive.[45]

DISCUSSION

This study demonstrates that MPTP opening is critical to experimental AP, mediating impaired ATP production, defective autophagy, zymogen activation, inflammatory responses and necrosis (figure 8), features of AP at molecular, cellular and whole organism levels.[1] Our previous work identified metabolic effects of MPTP opening specific to ethanol. Here we have established the general significance of MPTP opening as a central mechanism in the pathogenesis of AP, and the primary role of calcium overload in this. The patch clamp data show how tight control of cytosolic calcium elevations essential to normal stimulus-secretion coupling by IP_3Rs and RyRs[4] is lost in Wt but maintained in *Ppif*$^{-/-}$ pancreatic acinar cells, which preserve ATP supply and clear calcium more effectively. Coupling of endoplasmic reticulum IP_3Rs and RyRs with outer mitochondrial membranes tightly localises high calcium concentrations,[46] but may expose mitochondria to abnormal calcium release, despite modulation by Bcl-2 family proteins.[7] Here we have shown that pancreatitis toxins cause abnormal release of calcium via IP_3Rs and RyRs that overloads pancreatic acinar mitochondria, which are markedly sensitive to calcium signals.[23] The mitochondrial calcium overload induces high conductance MPTP opening and dissipates $\Delta\psi_m$, initiating collapse of ATP production, diminished calcium clearance, PGAM5 activation and subsequent necrosis. Importantly for a disease without specific treatment, pharmacological MPTP inhibition[29 47] administered after AP induction came close to preventing all injury, notably in the clinically relevant TLCS-AP.

For more than a century following an original postulate by Chiari,[48] pancreatitis has been viewed as an autodigestive disease consequent on pathological zymogen activation.[3 34 38 39 45] In experimental AP, zymogens are activated inside acinar cells within minutes of toxin exposure,[1 3 30 41] which this work has shown to result from induction of the MPTP, caused by and contributing to calcium overload. Sustained calcium overload may activate degradative calpains, phospholipases or other enzymes[17] and damage zymogen granules, inducing autophagic[41] and/or endolysosomal[49] responses that activate digestive enzymes. Such activation was not completely prevented by MPTP inhibition, however, likely from global cytosolic calcium overload that was seen to be more effectively cleared in *Ppif*$^{-/-}$ cells, without which overload no enzyme activation occurs.[30] Nevertheless, intracellular expression of trypsin per se without mitochondrial injury leads to apoptotic not necrotic pathway activation[45] and trypsinogen activation does not appear necessary for either local or systemic inflammation;[50] knockout of cathepsin B greatly reduces trypsinogen activation with little effect on serum IL-6 or lung injury.[39] Hereditary pancreatitis caused by cationic trypsinogen gene mutations rarely features clinically significant pancreatic necrosis;[51 52] further, systemic protease inhibition has had little success as a clinical strategy,[1] suggesting that while zymogen activation contributes, it is not the critical driver of AP. This study, however, shows that MPTP opening triggers defective autophagy, while inhibition of MPTP opening preserved ATP supply, increased the efficiency of autophagy and decreased zymogen activation. Together with major effects of MPTP opening on PGAM5 activation that implements necrosis,[19 37] and on local and systemic inflammatory responses, these findings now place mitochondrial injury centrally in AP.

Our new data show that in pancreatic acinar cells IP_3Rs and RyRs are vulnerable to specific toxins that markedly increase their calcium channel open-state probabilities. Toxic transformation of calcium channel function induced pancreatic acinar cell necrosis through calcium-dependent formation of the MPTP, with diminished ATP production the critical consequence. Toxic

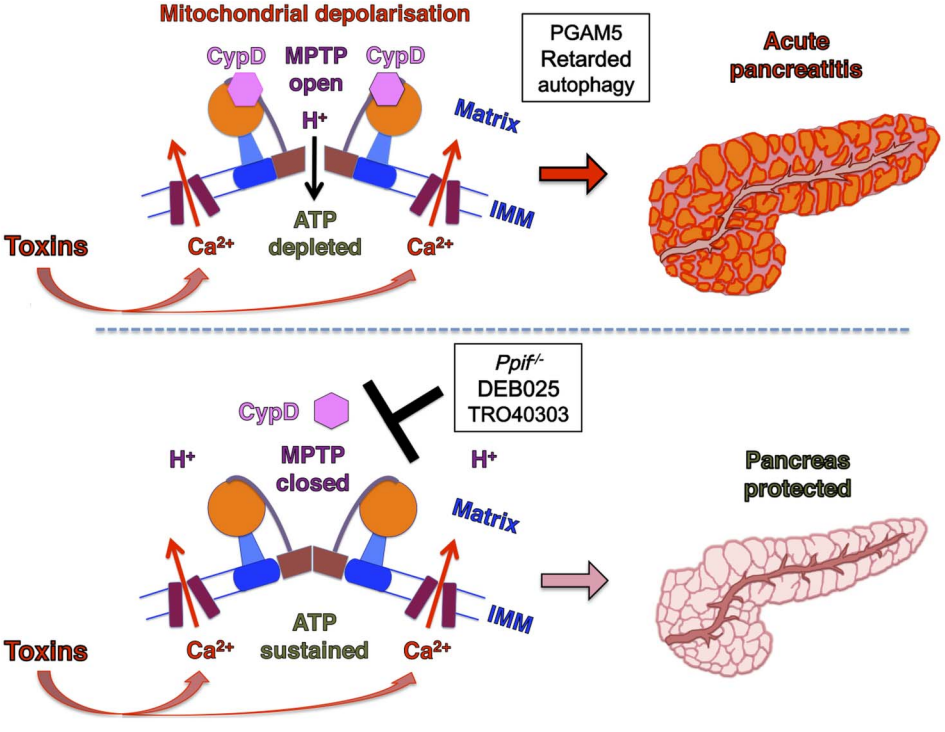

Figure 8 Summary diagram: the mitochondrial permeability transition pore (MPTP) plays a critical role in the development of acute pancreatitis. Exposure to pancreatic toxins leads to a sustained rise in cytoplasmic calcium that crosses the inner mitochondrial membrane (IMM) to enter the mitochondrial matrix. Consequent cyclophilin D (CypD) activation promotes MPTP opening across the IMM, causing mitochondrial depolarisation and impaired ATP production. These induce PGAM5 activation and retarded autophagy, downstream mechanisms in acute pancreatitis (upper panel). When MPTP opening is inhibited by genetic (Ppif$^{-/-}$) or pharmacological means (DEB025 or TR040303), mitochondrial membrane potential is preserved and ATP production sustained. This maintains the integrity of pancreatic acinar cells that clear calcium more effectively and prevents the development of acute pancreatitis (lower panel) (MPTP drawn after reference 14).

transformation by different toxins was specific to different second messengers, identifying potential for a variety of deleterious effects. ATP deficiency may be further exacerbated by fatty acids released on hydrolysis of FAEEs or triglycerides,[53] which may inhibit beta oxidation.[6] Without sufficient ATP, cytosolic calcium overload produces a vicious circle in which high-affinity, low-capacity sarcoendoplasmic reticulum calcium transport ATPase (SERCA) and plasma membrane calcium ATPase (PMCA) pump clearance of cytosolic calcium is impaired, further mitochondrial injury sustained and necrotic cell death accelerated.[6 12] Although the toxicity of cytosolic calcium overload depends on calcium store refilling from outside the cell,[30 54] specific second messenger receptor blockade demonstrated calcium overload to be due completely to release from their calcium channels, not direct effects of toxins on calcium entry or extrusion.

Whereas the vast majority of previous studies undertaken to determine mechanisms and/or new targets in AP have used only one model, our four models are broadly representative of a range of aetiologies, including biliary (TLCS-AP), hyperstimulation (CER-AP), ethanolic (FAEE-AP) and amino acid-induced (CDE-AP).[1 55] Our findings in experimental AP are entirely consistent with those made in isolated mitochondria and cells, identifying a generalised mechanism of pancreatic injury and necrosis, confirmed in murine and human pancreatic acinar cells, pancreas lobules and tissue slices. Pancreatic necrosis drives the inflammasome,[56] which can be induced by MPTP opening[57] and is part of the systemic inflammatory response contributing to multiple organ failure.[2] Further pancreatic injury is driven through tumour necrosis factor receptor activation that also promotes MPTP opening[58] and calcium deregulation, activating calcineurin and NFAT.[59] Our data link necrosis and inflammation directly, highlighting the potential of the MPTP as a drug target for AP.

Author affiliations
[1]NIHR Liverpool Pancreas Biomedical Research Unit, Royal Liverpool University Hospital, Liverpool, UK
[2]Institute of Translational Medicine, University of Liverpool, Liverpool, UK
[3]Veterans Affairs Greater Los Angeles Healthcare System, University of California Los Angeles and Southern California Research Center for Alcoholic Liver and Pancreatic Diseases and Cirrhosis, Los Angeles, California, USA
[4]Institute of Theoretical and Experimental Biophysics, Russian Academy of Sciences, Pushchino, Russia
[5]Department of Integrated Traditional and Western Medicine, Sichuan Provincial Pancreatitis Centre, West China Hospital, Sichuan University, Chengdu, People's Republic of China
[6]Debiopharm Research and Manufacturing S.A., Lausanne, Switzerland
[7]Trophos S.A., Marseille, France
[8]Howard Hughes Medical Institute, Children's Hospital Medical Center, Cincinnati, Ohio, USA
[9]Cardiff School of Biosciences, University of Cardiff, Cardiff, Wales, UK

Acknowledgements The authors thank Dr George Perides and Professor Michael Steer who taught R.M. techniques for TLCS-AP.

Collaborators The authors are indebted to members of the NIHR Pancreas BRU: Diane Latawiec for technical assistance, Dayani Rajamanoharan for pancreatic lobule assays, Euan Mclaughlin for whole cell assays with caffeine and Paula Ghaneh, Christopher Halloran, John P Neoptolemos and Michael GT Raraty for provision of human pancreas tissue samples. The authors wish to thank Dr Samuel W. French (Harbor-UCLA Medical Center, Torrance, CA) for providing electron micrographs that show mitochondrial damage in CER-AP.

Contributors RM and OAM are co-first authors. ASG and RS are co-senior authors. ASG and RS designed and supervised the study. RM, OAM, IVO, WH, JM, MC, MAJ, LW, DMB, MCC and MA performed the experiments. BG, RMP, SS, AVT, OHP, SJP, IG, JDM, DNC and the NIHR Pancreas BRU made technical and scientific contributions. RS, ASG, IG, RM and OAM wrote the paper.

Funding This work was supported by US Veterans Administration Merit Review (ASG), NIH grants R01DK59936 (ASG) and R01AA19730 (IG and OAM), Southern California Research Center for Alcoholic Liver and Pancreatic Diseases (SJP and ASG), American Gastroenterological Association Foundation Designated Research Scholar Award in Pancreatitis (OAM), Russian Federation BR grant 09-04-00739 (IVO), UK/China Postgraduate Research Scholarship for Excellence (WH), Liverpool China Scholarship Council Award (LW), CORE, UK (RM, JM, MAJ), UK Medical Research Council (DMB, MC, MCC, OHP, AVT, DNC and RS), Royal College of Surgeons of England (MAJ) and UK NIHR Biomedical Research Unit Funding Scheme (MA, AVT, DNC and RS).

Competing interests BG is an employee of Debiopharm Research and Manufacturing S.A., who supplied DEB025; RMP and SS are employees of Trophos SA, who supplied TRO40303; RS has received research funding from Debiopharm Research and Manufacturing S.A. and has acted as a consultant for Novartis International A.G.

Ethics approval Human pancreatic samples were donated by patients undergoing surgery for left-sided or unobstructing pancreatic tumours as approved by Liverpool Adult Local Research Ethics Committee (Ref: 03/12/242/A). Animal protocols were approved by UK Home Office (PPL 40/3320) and animal research committee of Veterans Affairs Greater Los Angeles Healthcare System, as per NIH guidelines..

Provenance and peer review Not commissioned; externally peer reviewed.

Data sharing statement Further unpublished data identified in the text of this article can be made available to bona fide researchers after communication with the corresponding author.

REFERENCES

1 Pandol SJ, Saluja AK, Imrie CW, *et al*. Acute pancreatitis: bench to bedside. *Gastroenterology* 2007;132:1127–51; erratum: *ibid*, 133;1056.
2 Petrov MS, Shanbhag S, Chakraborty M, *et al*. Organ failure and infection of pancreatic necrosis as determinants of mortality in patients with acute pancreatitis. *Gastroenterology* 2010;139:813–20.
3 Leach SD, Modlin IM, Scheele GA, *et al*. Intracellular activation of digestive zymogens in rat pancreatic acini. Stimulation by high doses of cholecystokinin. *J Clin Invest* 1991;87:362–6.
4 Petersen OH, Tepikin AV. Polarized calcium signaling in exocrine gland cells. *Annu Rev Physiol* 2008;70:273–99.
5 Schild L, Matthias R, Stanarius A, *et al*. Induction of permeability transition in pancreatic mitochondria by cerulein in rats. *Mol Cell Biochem* 1999;195:191–7.
6 Criddle DN, Murphy J, Fistetto G, *et al*. Fatty acid ethyl esters cause pancreatic calcium toxicity via inositol trisphosphate receptors and loss of ATP synthesis. *Gastroenterology* 2006;130:781–93.
7 Sung K-F, Odinokova IV, Mareninova OA, *et al*. Prosurvival Bcl-2 proteins stabilize pancreatic mitochondria and protect against necrosis in pancreatitis. *Exp Cell Res* 2009;315:1975–89.
8 Voronina SG, Barrow SL, Simpson AW, *et al*. Dynamic changes in cytosolic and mitochondrial ATP levels in pancreatic acinar cells. *Gastroenterology* 2010;138:1976–87.
9 Shalbueva N, Mareninova OA, Gerloff A, *et al*. Effects of oxidative alcohol metabolism on the mitochondrial permeability transition pore and necrosis in a mouse model of alcoholic pancreatitis. *Gastroenterology* 2013;144:437–46.
10 Lerch MM, Halangk W, Mayerle J. Preventing pancreatitis by protecting the mitochondrial permeability transition pore. *Gastroenterology* 2013;144:265–9.
11 Huang W, Booth DM, Cane MC, *et al*. Fatty acid ethyl ester synthase inhibition ameliorates ethanol-induced Ca2+-dependent mitochondrial dysfunction and acute pancreatitis. *Gut* 2014;63:1313–24.
12 Booth DM, Murphy JA, Mukherjee R, *et al*. Reactive oxygen species induced by bile acid induce apoptosis and protect against necrosis in pancreatic acinar cells. *Gastroenterology* 2011;140:2116–25.
13 Halestrap AP, Richardson AP. The mitochondrial permeability transition: a current perspective on its identity and role in ischaemia/reperfusion injury. *J Mol Cell Cardiol* 2015;78:129–41.
14 Giorgio V, von Stockum S, Antoniel M, *et al*. Dimers of mitochondrial ATP synthase form the permeability transition pore. *Proc Natl Acad Sci USA* 2013;110:5887–92.
15 Alavian KN, Beutner G, Lazrove E, *et al*. An uncoupling channel within the c-subunit ring of the F_1F_O ATP synthase is the mitochondrial permeability transition pore. *Proc Natl Acad Sci U S A* 2014;111:10580–5.
16 Elrod JW, Wong R, Mishra S, *et al*. Cyclophilin D controls mitochondrial pore-dependent Ca(2+) exchange, metabolic flexibility, and propensity for heart failure in mice. *J Clin Invest* 2010;120:3680–7.
17 Vandenabeele P, Galluzzi L, Vanden Berghe T, *et al*. Molecular mechanisms of necroptosis: an ordered cellular explosion. *Nat Rev Mol Cell Biol* 2010;11:700–14.

18 Gukovskaya AS, Gukovsky I, Jung Y, *et al*. Cholecystokinin induces caspase activation and mitochondrial dysfunction in pancreatic acinar cells. Roles in cell injury processes of pancreatitis. *J Biol Chem* 2002;277:22595–604.
19 Wang Z, Jiang H, Chen S, *et al*. The mitochondrial phosphatase PGAM5 functions at the convergence point of multiple necrotic death pathways. *Cell* 2012;148:228–43.
20 Baines CP, Kaiser RA, Purcell NH, *et al*. Loss of cyclophilin D reveals a critical role for mitochondrial permeability transition in cell death. *Nature* 2005;434:658–62.
21 Mizushima N, Yamamoto A, Matsui M, *et al*. In vivo analysis of autophagy in response to nutrient starvation using transgenic mice expressing a fluorescent autophagosome marker. *Mol Biol Cell* 2004;15:1101–11.
22 Murphy J, Criddle DN, Sherwood M, *et al*. Direct activation of cytosolic Ca2+ signaling and enzyme secretion by cholecystokinin in human pancreatic acinar cells. *Gastroenterology* 2008;135:632–41.
23 Odinokova IV, Sung KF, Mareninova OA, *et al*. Mechanisms regulating cytochrome c release in pancreatic mitochondria. *Gut* 2009;58:431–42.
24 Lossi L, Alasia S, Salio C, *et al*. Cell death and proliferation in acute slices and organotypic cultures of mammalian CNS. *Prog Neurobiol* 2009;88:221–45.
25 Cancela JM, Van Coppenolle F, Galione A, *et al*. Transformation of local Ca2+ spikes to global Ca2+ transients: the combinatorial roles of multiple Ca2+ releasing messengers. *EMBO J* 2002;21:909–19.
26 Mareninova OA, Sung KF, Hong P, *et al*. Cell death in pancreatitis: caspases protect from necrotizing pancreatitis. *J Biol Chem* 2006;281:3370–81.
27 Laukkarinen JM, Van Acker GJ, Weiss ER, *et al*. A mouse model of acute biliary pancreatitis induced by retrograde pancreatic duct infusion of Na-taurocholate. *Gut* 2007;56:1590–8.
28 Lombardi B, Estes LW, Longnecker DS. Acute necrotizing pancreatitis (massive necrosis) with fat necrosis induced in mice by DL-ethionine fed with a choline-deficient diet. *Am J Pathol* 1975;79:465–80.
29 Zorof DB, Juhaszova M, Yaniv Y, *et al*. Regulation and pharmacology of the mitochondrial permeability transition pore. *Cardiovasc Res* 2009;83:213–25.
30 Raraty M, Ward J, Erdemli G, *et al*. Calcium-dependent enzyme activation and vacuole formation in the apical granular region of pancreatic acinar cells. *Proc Natl Acad Sci USA* 2000;97:13126–31.
31 Voronina SG, Barrow SL, Gerasimenko OV, *et al*. Effects of secretagogues and bile acids on mitochondrial membrane potential of pancreatic acinar cells: comparison of different modes of evaluating DeltaPsim. *J Biol Chem* 2004;279:27327–38.
32 Schaller S, Paradis S, Ngoh GA, *et al*. TRO40303, a new cardioprotective compound, inhibits mitochondrial permeability transition. *J Pharmacol Exp Ther* 2010;333:696–706.
33 Gerasimenko JV, Flowerdew SE, Voronina SG, *et al*. Bile acids induce Ca2+ release from both the endoplasmic reticulum and acidic intracellular calcium stores through activation of inositol trisphosphate receptors and ryanodine receptors. *J Biol Chem* 2006;281:40154–63.
34 Husain SZ, Prasad P, Grant WM, *et al*. The ryanodine receptor mediates early zymogen activation in pancreatitis. *Proc Natl Acad Sci USA* 2005;102:14386–91.
35 Gerasimenko JV, Lur G, Sherwood MW, *et al*. Pancreatic protease activation by alcohol metabolite depends on Ca2+ release via acid store IP3 receptors. *Proc Natl Acad Sci USA* 2009;106:10758–63.
36 Gerasimenko JV, Gryshchenko O, Ferdek PE, *et al*. Ca2+ release-activated Ca2+ channel blockade as a potential tool in antipancreatitis therapy. *Proc Natl Acad Sci USA* 2013;110:13186–91.
37 Sekine S, Kanamaru Y, Koike M, *et al*. Rhomboid protease PARL mediates the mitochondrial membrane potential loss-induced cleavage of PGAM5. *J Biol Chem* 2012;287:34635–45.
38 Saluja A, Saluja M, Villa A, *et al*. Pancreatic duct obstruction in rabbits causes digestive zymogen and lysosomal enzyme colocalization. *J Clin Invest* 1989;84:1260–6.
39 Halangk W, Lerch MM, Brandt-Nedelev B, *et al*. Role of cathepsin B in intracellular trypsinogen activation and the onset of acute pancreatitis. *J Clin Invest* 2000;106:773–81.
40 Neoptolemos JP, Kemppainen EA, Mayer JM, *et al*. Early prediction of severity in acute pancreatitis by urinary trypsinogen activation peptide: a multicentre study. *Lancet* 2000;355:1955–60.
41 Mareninova OA, Hermann K, French SW, *et al*. Impaired autophagic flux mediates acinar cell vacuole formation and trypsinogen activation in rodent models of acute pancreatitis. *J Clin Invest* 2009;119:3340–55.
42 Gukovskaya AS, Gukovsky I. Autophagy and pancreatitis. *Am J Physiol Gastrointest Liver Physiol* 2012;303:G993–1003.
43 Lüthen R, Niederau C, Grendell JH. Intrapancreatic zymogen activation and levels of ATP and glutathione during caerulein pancreatitis in rats. *Am J Physiol* 1995;268: G592–604.
44 Zhang H, Neuhöfer P, Song L, *et al*. IL-6 trans-signaling promotes pancreatitis-associated lung injury and lethality. *J Clin Invest* 2013;123:1019–31.
45 Gaiser S, Daniluk J, Liu Y, *et al*. Intracellular activation of trypsinogen in transgenic mice induces acute but not chronic pancreatitis. *Gut* 2011;60:1379–88.
46 Rizzuto R, Pinton P, Carrington W, *et al*. Close contacts with the endoplasmic reticulum as determinants of mitochondrial Ca2+ responses. *Science* 1998;280:1763–6.
47 Naoumov NV. Cyclophilin inhibition as potential therapy for liver diseases. *J Hepatol* 2014;61:1166–74.
48 Chiari H. Uber die Selbstverdauung des menschlichen Pankreas. *Z Heilk* 1896;17:69–96.
49 Sherwood MW, Prior IA, Voronina SG, *et al*. Activation of trypsinogen in large endocytic vacuoles of pancreatic acinar cells. *Proc Natl Acad Sci USA* 2007;104:5674–9.
50 Dawra R, Sah RP, Dudeja V, *et al*. Intra-acinar trypsinogen activation mediates early stages of pancreatic injury but not inflammation in mice with acute pancreatitis. *Gastroenterology* 2011;141:2210–17.
51 Whitcomb DC, Gorry MC, Preston RA, *et al*. Hereditary pancreatitis is caused by a mutation in the cationic trypsinogen gene. *Nat Genet* 1996;14:141–5.
52 Howes N, Lerch MM, Greenhalf W, *et al*. Clinical and genetic characteristics of hereditary pancreatitis in Europe. *Clin Gastroenterol Hepatol* 2004;2: 252–61.
53 Navina S, Acharya C, Delany JP, *et al*. Lipotoxicity causes multisystem organ failure and exacerbates acute pancreatitis in obesity. *Sci Transl Med* 2011;3:107ra110.
54 Kim MS, Hong JH, Li Q, *et al*. Deletion of TRPC3 in mice reduces store-operated Ca^{2+} influx and the severity of acute pancreatitis. *Gastroenterology* 2009;137: 1509–17.
55 Simon P, Weiss FU, Zimmer KP, *et al*. Acute and chronic pancreatitis in patients with inborn errors of metabolism. *Pancreatology* 2001;5:448–56.
56 Hoque R, Sohail M, Malik A, *et al*. TLR9 and the NLRP3 inflammasome link acinar cell death with inflammation in acute pancreatitis. *Gastroenterology* 2011;141:358–69.
57 Nakahira K, Haspel JA, Rathinam VA, *et al*. Autophagy proteins regulate innate immune response by inhibiting NALP3 inflammasome-mediated mitochondrial DNA release. *Nat Immunol* 2011;12:222–30.
58 He S, Wang L, Miao L, *et al*. Receptor interacting protein kinase-3 determines cellular necrotic response to TNF-alpha. *Cell* 2009;137:1100–11.
59 Muili KA, Wang D, Orabi AI, *et al*. Bile acids induce pancreatic acinar cell injury and pancreatitis by activating calcineurin. *J Biol Chem* 2013;288:570–80.

Correction: *Mechanism of mitochondrial permeability transition pore induction and damage in the pancreas: inhibition prevents acute pancreatitis by protecting production of ATP*

Mukherjee R, Mareninova OA, Odinokova, *et al*. Mechanism of mitochondrial permeability transition pore induction and damage in the pancreas: inhibition prevents acute pancreatitis by protecting production of ATP. *Gut* 2016;65:1333-46. doi: 10.1136/gutjnl-2014-308553.

The authors wish to correct the collaborator statement in the paper. It should read as follows:

Collaborators: The authors are indebted to members of the NIHR Pancreas BRU: Diane Latawiec for technical assistance, Dayani Rajamanoharan for pancreatic lobule assays, Euan Mclaughlin for whole cell assays with caffeine and Paula Ghaneh, Christopher Halloran and Michael GT Raraty for provision of human pancreas tissue samples. The authors wish to thank Dr Samuel W French (Harbor-UCLA Medical Center, Torrance, CA) for providing electron micrographs that show mitochondrial damage in CER-AP.

OPEN ACCESS

Gut 2019;**68**:1136. doi:10.1136/gutjnl-2014-308553corr1

Supplementary Methods

Pancreas tissue slices and lobules. Human pancreas tissue was set in 10% gelatine and sliced with a Leica VT1200 Vibratome (Leica Microsystems Gmbh) at ~150 µm thickness. Slices were loaded with TMRM (10 µM, 20 min, dequench mode[23]), washed, and measured using a PolarStar Omega BMG Labtech microplate reader (excitation 540 nm, emission 590 nm). Murine pancreas lobules were dissociated manually and placed in (mM): 140 NaCl, 4.7 KCl, 1.13 $MgCl_2$, 1 $CaCl_2$, 10 D-glucose, 10 HEPES (adjusted to pH 7.35 using NaOH).

Isolated mitochondria responses. Measurements were made on mitochondria in *medium A* containing 250 mM sucrose, 22 mM KCl, 22 mM triethanolamine (pH 7.4), 3 mM $MgCl_2$, 5 mM KH_2PO_4; or *medium B* containing 100 mM KCl, 30 mM 3-morpholinopropanesulfonic acid (pH 7.2), 3 mM $MgCl_2$, 5 mM KH_2PO_4, and 10 mM calcium/EGTA buffers; 10 mM succinate was used as the respiratory substrate. Oxygen consumption was measured using a Clark-type electrode (Instech Lab) and oxygen meter (Yellow Springs Instruments). Membrane potential was monitored in presence of 1 µM tetraphenyl phosphonium (TPP^+) with TPP^+-sensitive electrode[9,26].

Electron microscopy. Pancreatic tissue was cut into 1 mm cubes and fixed overnight at 4^{o}C in 2.5% glutaraldehyde, 0.15 M sodium cacodylate (pH 7.4). After post-fixation in 1% OsO_4 followed by uranyl acetate, tissue was dehydrated in ethanol and embedded in epoxy resin. 100 nm thick sections were examined in a Hitachi 600 electron microscope.

Immunofluorescence. For immunolabeling, murine pancreata were dissected and fixed as described[37]. Images were acquired with a Zeiss LSM

710 confocal microscope using x 63 objective. Nuclei were counterstained with DAPI.

Enzyme activity, ATP and IL-6 determination. Trypsin activity was measured in homogenized cells/tissue, using Boc-Gln-Ala-Arg-AMC substrate converted by trypsin to a fluorescent product (excitation 380 nm, emission 440 nm) [37]. Serum amylase was measured by Hitachi 707 (Antech Diagnostics) or Roche Analyzer (Roche), and serum IL-6 levels by Quantikine ELISA (R&D Systems). ATP levels were measured in pancreatic homogenates by luciferin/luciferase-based ATP determination kit (Molecular Probes)[7], with TD 20/20 luminometer (Turner Designs).

Myeloperoxidase assay. Myeloperoxidase activity was measured by a bromide-dependent fluorometric assay[41]. Pancreatic tissue was homogenized, resuspended in 100 mM potassium phosphate buffer (pH 5.4) containing 0.5% hexadecyltrimethyl ammonium bromide, 10 mM EDTA and protease inhibitors, freeze-thawed three times, sonicated for 30 sec and centrifuged for 15 min at 16,000 $\times$ g. Myeloperoxidase activity was measured in supernatants mixed with 3,3,5,5-tetramethylbenzidine as substrate (1.6 mM, final) with freshly added H_2O_2 (3 mM, final; absorbance at 655 nm for 3 min at 30 sec intervals). Activity was calculated by standard curve and expressed as units/mg protein or normalized to control.

Immunoblot analysis. Immunoblotting of pancreatic tissue, isolated mitochondrial homogenates, membrane or cytosolic fractions was as described[44]. Protein concentration was determined by Bradford assay (Bio-Rad Laboratories). Blots were visualized by enhanced chemiluminescence detection kit (Pierce). Band intensities were quantified by densitometry using

Scion imaging software (Scion Corporation) or FluorChem HD2 imaging system (Alpha Innotech). Cytochrome c release was measured by immunoblot[44].

Chemicals and reagents. CCK-8 was from American Peptide; caerulein, Peninsula Laboratories; Boc-Gln-Ala-Arg-AMC, Peptides International; TMRM, Invitrogen other fluorescent dyes, Molecular Probes; antibody against cytochrome c, BD Biosciences; anti-COX IV, Molecular Probes; anti-cyclophilin D, Affinity Bioreagents; anti-trypsin, Chemicon International; anti-PGAM5, Santa Cruz Biotechnology Inc; anti-LC3B and anti-SQSTM1/p62, Cell Signaling Technology. Purified trypsin was from Worthington; calcium/EGTA buffer kit; Molecular Probes; IL-6 ELISA kit, R&D Systems Europe Ltd; other reagents, Sigma Chemical; D-MeAla^3-EtVal^4-cyclosporin (Alisporivir, DEB025), Debiopharm S.A.; 3,5-Seco-4-nor-cholestan-5-one oxime-3-ol (TRO40303), Trophos S.A..

List of Abbreviations:

ACh:	acetylcholine
ADP:	adenosine diphosphate
AP:	acute pancreatitis
ATP:	adenosine triphosphate
BAPTA:	1,2-bis(o-aminophenoxy)ethane-N,N,N',N'-tetraacetic acid
Bcl2:	B-cell lymphoma 2
BKA:	bongkrekic acid
CCCP:	carbonyl cyanide *m*-chlorophenyl hydrazone
CCK:	cholecystokinin
CDE:	choline-deficient ethionine-supplemented
CER:	caerulein
CYA:	cyclosporin A
CypD:	cyclophilin D
DCFDA:	dichlorodihydrofluorescein diacetate acetyl ester
DEB025:	alisporivir
EGTA:	ethylene glycol tetraacetic acid
ELISA:	enzyme-linked immunosorbent assay
ERK:	extracellular-signal regulated kinase
FAEE:	fatty acid ethyl ester
GFP:	green fluorescent protein
H&E:	haematoxylin and eosin
ICl_{Ca}:	calcium-activated Cl^- currents
IMM:	inner mitochondrial membrane
IP_3:	inositol trisphosphate
IP_3R:	inositol trisphosphate receptor
LC3:	microtubule-associated protein 1A/1B-light chain 3
MEN:	menadione
MPTP:	mitochondrial permeability transition pore
NAADP:	nicotinic acid adenine dinucleotide phosphate
NAD(P)H:	nicotinamide adenine dinucleotide (phosphate)
NFAT:	nuclear factor of activated T-cells
PGAM5:	phosphoglycerate mutase family member 5
PI:	propidium iodide
POA:	palmitoleic acid
POAEE:	palmitoleic acid ethyl ester
PPI:	peptidyl-prolyl isomerase
Ppif:	peptidyl-prolyl isomerase F (also known as D) gene
R110:	rhodamine 110
ROS:	reactive oxygen species
RyR:	ryanodine receptor
SO:	sytox orange
SQSTM1:	sequestosome 1 (also known as p62)
TLCS:	taurolithocholic acid sulphate
TMRM:	tetramethyl rhodamine methyl ester
TPP:	tetraphenyl phosphonium
TRO40303:	3,5-Seco-4-nor-cholestan-5-one oxime-3-ol
TUNEL:	terminal deoxynucleotidyl transferase dUTP nick end labeling
Wt:	wild type

Figure S1

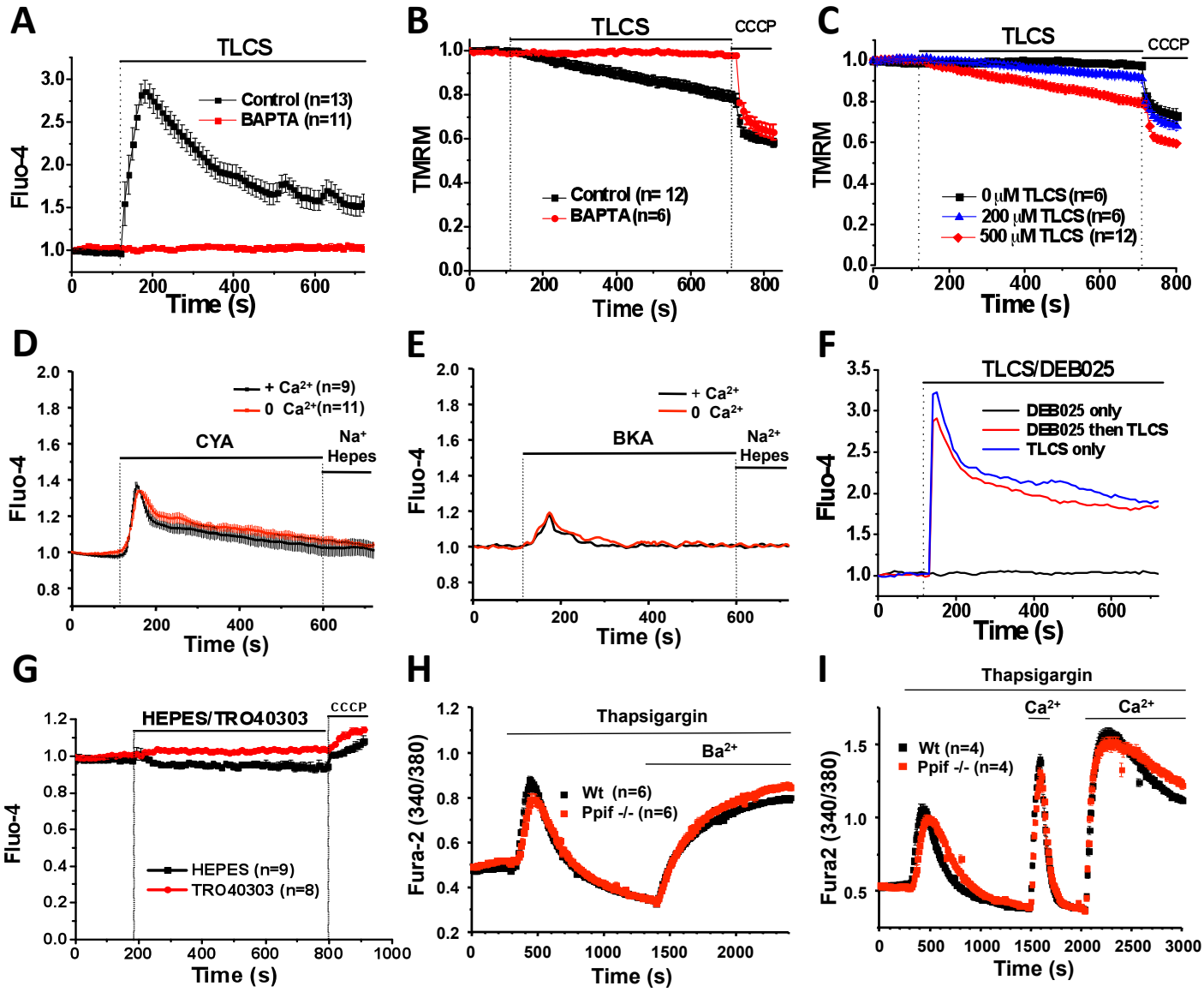

Figure S1. Effects of TLCS and pharmacological or genetic MPTP inhibition on cytosolic calcium (Fluo-4 or Fura-2) and mitochondrial membrane potential (TMRM) responses of murine pancreatic acinar cells (mean ± s.e.m. ratio to basal, F/F_0; n = no. of experiments, each with many cells). (**A**) Effect of preloading with calcium chelator BAPTA on calcium and (**B**) $\Delta\psi_m$ responses to TLCS (500 µM) in comparison to cells without BAPTA. (**C**) Effect of TLCS on $\Delta\psi_m$ was dose dependent; the higher the concentration of TLCS, the greater the fall of $\Delta\psi_m$. (**D**) CYA-induced intracellular calcium release on first application of CYA, without (100 nM EGTA) or with extracellular calcium; (**E**) typical traces of BKA-induced calcium release without (100 nM EGTA) or with calcium. (**F**) DEB025 alone induced no cytosolic calcium change; DEB025 as pre-treatment followed by TLCS (labelled: DEB025 then TLCS) resulted in the same calcium changes as with TLCS only. (**G**) TRO40303 did not affect cytosolic calcium levels (CCCP protonophore control). (**H**) Calcium store depletion with thapsigargin (20 µM) in zero Ca^{2+} (100 nM EGTA) followed by extracellular barium (10 mM) entry (which is not extruded) showing similar entry rates in Wt and *Ppif*$^{-/-}$ cells confirmed in (**I**) with similar store depletion in zero Ca^{2+} followed by extracellular calcium (5 mM) entry, extrusion and re-entry in Wt and *Ppif*$^{-/-}$ cells (H and I mean ± s.e.m. ratio to basal, F/F_0).

Figure S2. Factors determining toxic globalisation of second messenger calcium release in response to pancreatitis toxins (*insets*, green Fluo-4 or red PI fluorescent cells, white bars = 10 μm). (**A**) *Top plot*: typical calcium spikes (Fluo-4, F/F_0, blue) elicited by patched IP_3 (1-10 μM) were transformed into global, prolonged elevations matched by ICl_{Ca} and non-specific cation currents upon POAEE (10 μM) application, inhibited by caffeine (Caf, pink); *middle plot*: sustained caffeine inhibition prevented toxic transformation and PI uptake from TLCS (10 μM) after IP_3; *bottom plot*: caffeine prevented toxic transformation and PI uptake from POAEE (10 μM) after IP_3. (**B**) Without external calcium, globalised signals (ICl_{Ca}) from POAEE after IP_3 decreased then disappeared, with no PI uptake. (**C**) TLCS (10 μM) induced toxic transformation of typical ICl_{Ca} elicited by cADPR (10 μM) not NAADP (100 nM) whereas POAEE (10 μM) induced toxic globalisation with NAADP (100 nM) not cADPR (10 μM); following transformation, early PI uptake prevented by patched ATP (red ICl_{Ca} with PI uptake, 0 mM ATP; black ICl_{Ca} no PI uptake, 4 mM ATP; two recordings superimposed in top and bottom plots). (**D**) *Top plot*: TLCS (10 μM) induced toxic globalisation of CCK-8- (1-5 pM) elicited calcium signals with PI uptake; *bottom plot*: control data showing no change in ATP (Mg Green) with patch, but decline after CCCP. (**E**) CCK-8 or ACh with TLCS (10 μM) or POAEE (10 μM) resulted in significantly increased PI uptake compared to TLCS (*$p<0.05$) or POAEE (†$p<0.05$) alone, without patch.

Figure S2

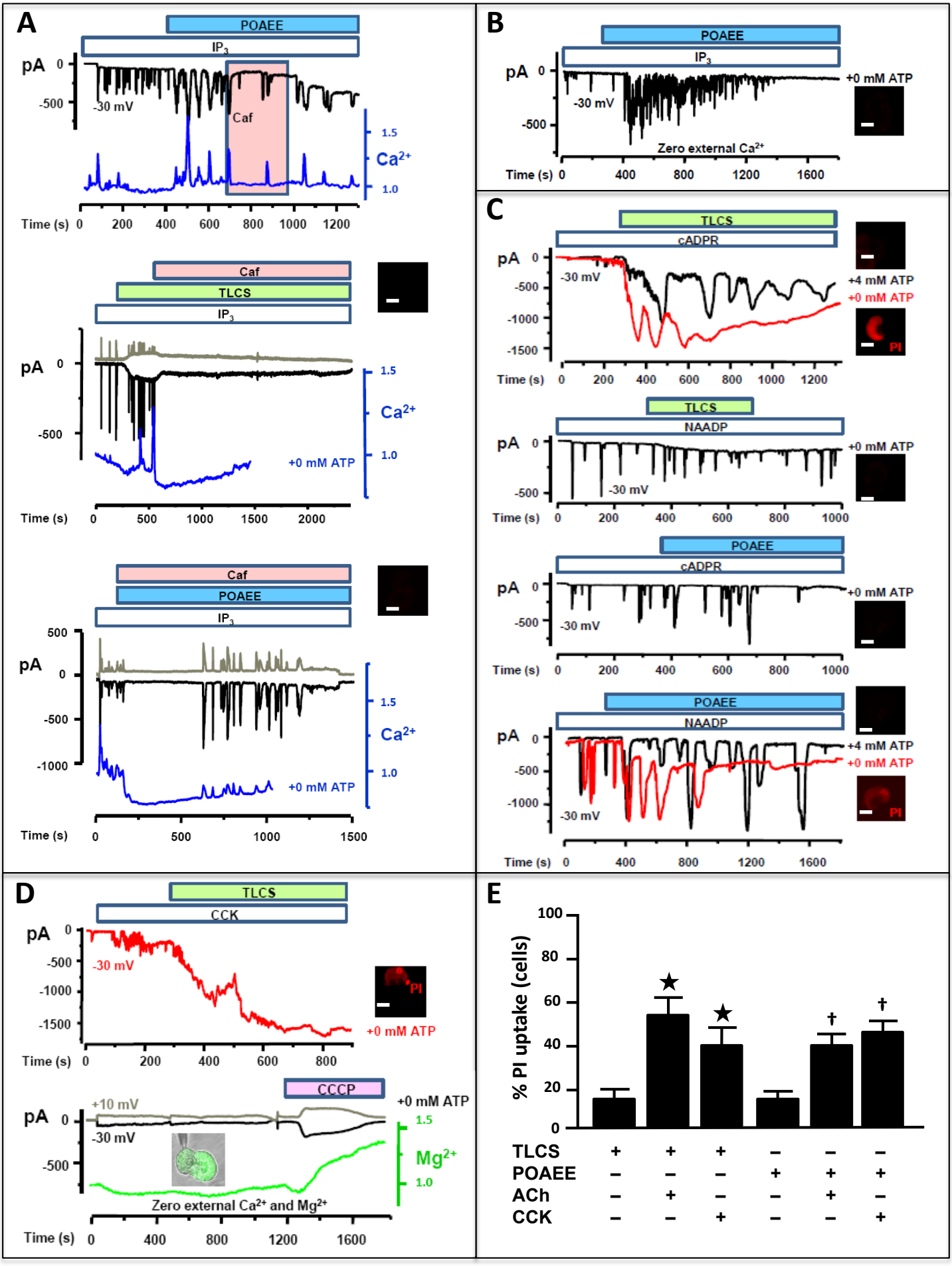
A
POAEE
IP3
pA
-30 mV
Caf
Ca2+
Time (s)
Caf
TLCS
IP3
+0 mM ATP
Caf
POAEE
IP3
B
POAEE
IP3
+0 mM ATP
-30 mV
Zero external Ca2+
Time (s)
C
TLCS
cADPR
+4 mM ATP
+0 mM ATP
PI
TLCS
NAADP
POAEE
cADPR
POAEE
NAADP
D
TLCS
CCK
PI
+0 mM ATP
CCCP
+10 mV
Mg2+
Zero external Ca2+ and Mg2+
E
% PI uptake (cells)
TLCS
POAEE
ACh
CCK

Figure S3

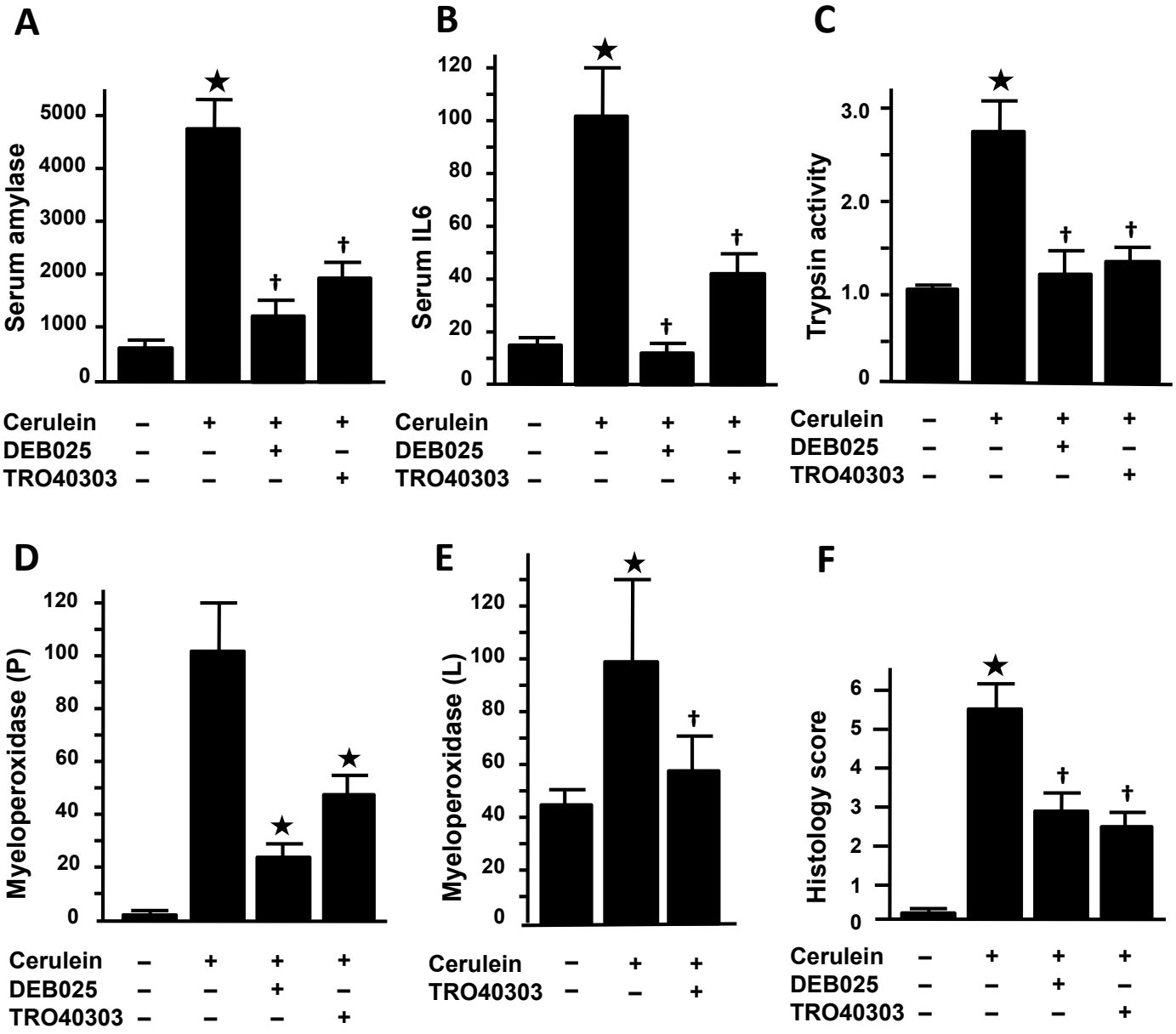

Figure S3. Pharmacological MPTP inhibition with DEB025 or TRO40303 markedly attenuates biochemical and histological responses of CER-AP in Wt mice. Characteristic elevations in CER-AP of (**A**) serum amylase (U/l) and (**B**) IL-6 (pg/ml), (**C**) pancreatic trypsin activity (normalized to saline controls at 1.0), (**D**) pancreatic (P) and (**E**) lung (L) myeloperoxidase activity (normalized to CER-AP at 100) and (**F**) histology scores (oedema, inflammatory infiltrate and necrosis) were all significantly reduced by treatment with DEB025 or TRO40303 (*$p<0.05$ for all elevations vs saline controls; †$p<0.05$ vs CER-AP without treatment).

Figure S4

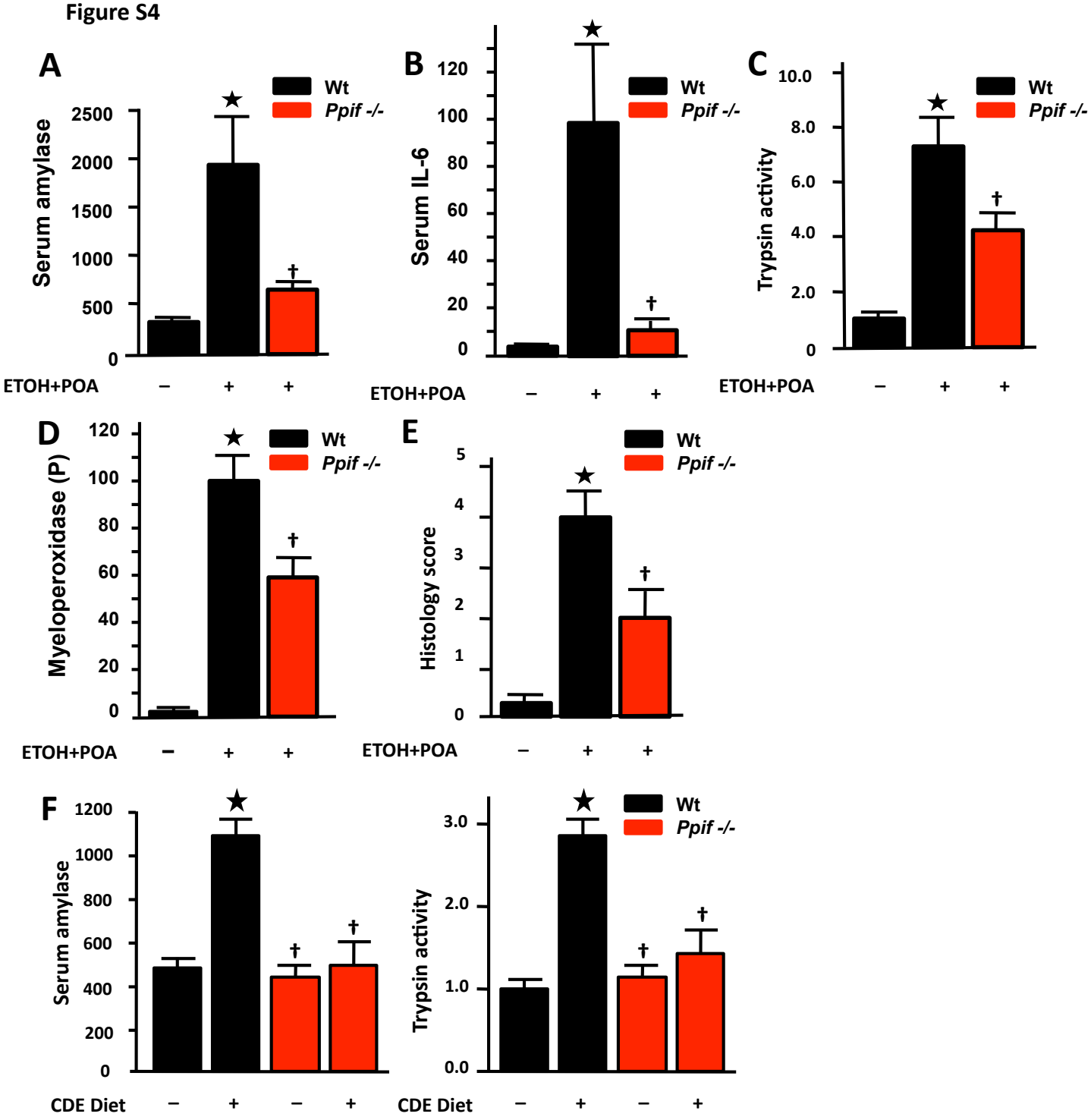

Figure S4. Genetic MPTP inhibition (*Ppif*$^{-/-}$) markedly attenuates biochemical and histological responses of FAEE-AP and CDE-AP. Characteristic elevations in FAEE-AP (Huang et al., 2013) of (**A**) serum amylase (U/l) and (**B**) IL-6 (pg/ml), (**C**) pancreatic trypsin activity (normalized to saline controls at 1.0), (**D**) pancreatic (P) myeloperoxidase activity (normalized to FAEE-AP at 100) and (**E**) histology scores (*p<0.05 vs Wt saline controls) were all significantly attenuated in *Ppif*$^{-/-}$ mice (†p<0.05 vs FAEE-AP in Wt). Characteristic elevations in CDE-AP of (**F**) serum amylase (*left*) and pancreatic trypsin activity (normalized to Wt controls receiving normal diet; *p<0.05 vs Wt controls, *right*) were abolished in *Ppif*$^{-/-}$ animals (†p<0.05 vs CDE-AP in Wt).

Table S1

Cells	Stimulus	Toxin	Caffeine	Pipette ATP	Globalisation[a]	PI uptake
Wt	1-10 μM IP_3	10 μM TLCS			6 of 6	5 of 6
Wt	1-10 μM IP_3	10 μM POAEE			9 of 9	8 of 9
Wt	1-10 μM IP_3	10 μM TLCS	20 mM		0 of 6	0 of 6[b]
Wt	1-10 μM IP_3	10 μM POAEE	20 mM		1 of 6	1 of 6[c]
Wt[d]	1-10 μM IP_3	10 μM TLCS			7 of 7[e]	1 of 7[c]
Wt[d]	1-10 μM IP_3	10 μM POAEE			7 of 7[e]	0 of 7[b]
Wt	1-10 μM IP_3	10 μM TLCS		4 mM	4 of 4[e]	0 of 4[c]
Wt	1-10 μM IP_3	10 μM POAEE		4 mM	4 of 4[e]	0 of 4[c]
$Ppif^{-/-}$	1-10 μM IP_3	10 μM TLCS			17 of 17[e]	0 of 17[b]
Wt	100nM NAADP	10 μM TLCS			1 of 13	N/A
Wt	100nM NAADP	10 μM POAEE			9 of 9	8 of 9
Wt	100nM NAADP	10 μM POAEE		4 mM	5 of 5[e]	0 of 5[b]
Wt	10 μM cADPR	10 μM TLCS			5 of 5	5 of 5
Wt	10 μM cADPR	10 μM TLCS		4 mM	4 of 4[e]	0 of 4[b]
Wt	10 μM cADPR	10 μM POAEE			0 of 12	N/A
Wt	1-5 pM CCK-8	10 μM TLCS			6 of 6	6 of 6
Wt	1-5 pM CCK-8	10 μM TLCS		4 mM	6 of 6[e]	0 of 6[b]
Wt	1-5 pM CCK-8	10 μM POAEE			7 of 7	7 of 7
Wt	1-5 pM CCK-8	10 μM POAEE		4 mM	5 of 5[e]	0 of 5[b]
Wt	20 nM ACh	10 μM TLCS			5 of 5	5 of 5
Wt	20 nM ACh	10 μM TLCS		4 mM	5 of 5[e]	0 of 5[b]
Wt	20 nM ACh	10 μM POAEE			6 of 6	6 of 6
Wt	20 nM ACh	10 μM POAEE		4 mM	6 of 6[e]	0 of 6[b]
Wt		200 μM TLCS			7 of 7	6 of 7
Wt		200 μM TLCS		4 mM	7 of 7[e]	0 of 7[b]
$Ppif^{-/-}$		200 μM TLCS			7 of 7[e]	0 of 7[b]

Table S1. Toxic globalisation of calcium signals and subsequent PI uptake elicited by quasi-physiological stimuli following application of pancreatitis toxins in Wt mouse pancreatic acinar cells, demonstrating protective effects of the IP_3R inhibitor caffeine or of no external calcium or of supplementary ATP in the pipette or of cyclophilin D knockout (*Ppif*$^{-/-}$; numbers of cells less than those given in main text as PI uptake was not tested in all cells from which ICI_{Ca} recordings were made).

[a]Globalisation characterised by transformation of apical into global calcium signals of >30 s duration.

[b]$p<0.01$ vs PI uptake in cells from respective Wt control group (i.e. calcium in external medium and no caffeine nor supplementary pipette ATP).

[c]$p<0.05$ vs PI uptake in cells from respective Wt control group (i.e. calcium in external medium with no caffeine nor supplementary pipette ATP).

[d]0 mM external calcium, demonstrating protection from PI uptake, as globalisation was not sustained in cells with external medium containing no calcium.

[e]Globalisation less marked/not sustained with no external calcium or with supplementary pipette ATP or in *Ppif*$^{-/-}$, showing return to baseline cytosolic calcium levels.